

Institutionen för systemteknik

Department of Electrical Engineering

Examensarbete

Electric Motors for Vehicle Propulsion

Examensarbete utfört i Fordonssystem
vid Tekniska högskolan vid Linköpings universitet
av

Martin Larsson

LiTH-ISY-EX--14/4743--SE

Linköping 2014



Linköpings universitet
TEKNISKA HÖGSKOLAN

Electric Motors for Vehicle Propulsion

Examensarbete utfört i Fordonssystem
vid Tekniska högskolan i Linköping
av

Martin Larsson

LiTH-ISY-EX--14/4743--SE

Handledare: **Christofer Sundström**
ISY, Linköpings universitet
Ingrid Sjunnesson
LeanNova Engineering AB, Trollhättan
Rudolf Brziak
LeanNova Engineering AB, Trollhättan

Examinator: **Mattias Krysander**
ISY, Linköpings universitet

Linköping, 24 January, 2014

	Avdelning, Institution Division, Department Division of Vehicular Systems Department of Electrical Engineering Linköpings universitet SE-581 83 Linköping, Sweden		Datum Date 2014-01-24
	Språk Language <input type="checkbox"/> Svenska/Swedish <input checked="" type="checkbox"/> Engelska/English <input type="checkbox"/> _____	Rapporttyp Report category <input type="checkbox"/> Licentiatavhandling <input checked="" type="checkbox"/> Examensarbete <input type="checkbox"/> C-uppsats <input type="checkbox"/> D-uppsats <input type="checkbox"/> Övrig rapport <input type="checkbox"/> _____	ISBN _____ ISRN LiTH-ISY-EX--14/4743--SE Serietitel och serienummer ISSN Title of series, numbering _____
URL för elektronisk version http://www.fs.isy.liu.se http://www.ep.liu.se			
Titel Title Elektriska motorer för fordonsframdrivning Electric Motors for Vehicle Propulsion			
Författare Martin Larsson Author			
Sammanfattning Abstract <p>This work is intended to contribute with knowledge to the area of electric motors for propulsion in the vehicle industry. This is done by first studying the different electric motors available, the motors suitable for vehicle propulsion are then divided into four different types to be studied separately. These four types are the direct current, induction, permanent magnet and switched reluctance motors. The design and construction are then studied to understand how the different types differ from each other and which differences that are of importance when it comes to vehicle propulsion. Since the amount of available data about different electric motors turned out to be small a tool was developed to use for collecting data from the sources available which can be for instance product sheets or articles with information about electric motors. This tool was then used to collect data that was used to create models for the different motor types. The created motor models for each motor type could then be used for simulating vehicles to investigate how the specific motor is suited for different vehicles and applications. The work also contains a summary of different electric motor comparison studies which makes it a good source of information during motor type selection in the process of designing an electric vehicle.</p>			
Nyckelord Keywords electric motor, vehicle propulsion, efficiency map, DC, induction, permanent magnet, switched reluctance			

Abstract

This work is intended to contribute with knowledge to the area of electric motors for propulsion in the vehicle industry. This is done by first studying the different electric motors available, the motors suitable for vehicle propulsion are then divided into four different types to be studied separately. These four types are the direct current, induction, permanent magnet and switched reluctance motors. The design and construction are then studied to understand how the different types differ from each other and which differences that are of importance when it comes to vehicle propulsion. Since the amount of available data about different electric motors turned out to be small a tool was developed to use for collecting data from the sources available which can be for instance product sheets or articles with information about electric motors. This tool was then used to collect data that was used to create models for the different motor types. The created motor models for each motor type could then be used for simulating vehicles to investigate how the specific motor is suited for different vehicles and applications. The work also contains a summary of different electric motor comparison studies which makes it a good source of information during motor type selection in the process of designing an electric vehicle.

Sammanfattning

Detta arbetet syftar till att bidra med kunskap inom området gällande elmotorer för framdrivning inom fordonsindustrin. Detta görs genom att först studera vilka elmotorer som finns tillgängliga, de motortyper som är lämpliga för fordonsframdrivning definieras som fyra grupper och studeras sedan var för sig. De fyra grupperna av motorer är likström, induktion, permanentmagnet och variabel reaktansmotorer. Konstruktionen av de olika motortyperna studeras för att förstå hur de skiljer sig åt och vilka skillnader som är av betydelse när de skall användas för att driva ett fordon. Eftersom tillgänglig information om de olika elmotortyperna visade sig vara begränsad så utvecklades också ett verktyg för att samla in data från de källor som finns publicerade i t.ex. produktblad eller olika artiklar. Detta verktyg användes sedan för att samla in den data som behövdes för att modellera de olika motortyperna. De framtagna modellerna över varje motortyp användes sedan för att göra simuleringar av fordon för att se hur väl den valda motorn fungerar för en specifik tillämpning och fordonstyp. Arbetet har också sammanfattat information från många olika jämförande studier när det gäller elmotorer för fordon vilket gör att mycket nyttig information finns samlad som kan användas vid valet av motortyp då man utvecklar ett elfordon.

Acknowledgments

This work has truly been an interesting journey where I had the privilege to work with something I have had great interest in since way back in time. That electric motors will play a key role in the future of transportation is something I am very convinced in since it is involved in all the probable solutions whether it is battery electric vehicles, hybrid vehicles or fuel cell vehicles. I want to thank my supervisors at LeanNova, Ingrid Sjunnesson and Rudolf Brziak, for giving me this opportunity and for all the help and interesting discussions during the work in Trollhättan. I want to thank my examiner at Linköping University, Mattias Krysander, and my supervisor, Christofer Sundström, for helping me with my questions and for the feedback during the report writing process.

Martin Larsson

Trollhättan, November 2013

Contents

1	Introduction	1
1.1	Background	1
1.2	Purpose and goals	1
1.3	Related research	2
1.4	Approach	3
1.5	Thesis contributions	5
1.6	Outline	5
2	Electric Motors	7
2.1	Electricity and magnetism	7
2.1.1	Magnetic fields	7
2.1.2	Producing a magnetic field	8
2.1.3	Magnetic flux density	9
2.1.4	Force on a conductor	10
2.1.5	Magnetic circuits	10
2.1.6	Reluctance torque	12
2.2	DC Motor Drives	13
2.2.1	Operation of the DC motor	13
2.2.2	Torque production	14
2.2.3	Electro Motoric Force	15
2.2.4	Torque/Speed control	16
2.3	Induction Motor Drives	19
2.3.1	Alternating current	19
2.3.2	The transformer	19
2.3.3	Operation of Induction motor	22
2.3.4	Equivalent circuit	25
2.3.5	Torque-Speed characteristics	25
2.3.6	Variable frequency control	27
2.4	Permanent Magnet Motor Drives	28
2.4.1	Operation of PM motors	28
2.4.2	Torque production	28
2.4.3	Torque-Speed characteristics	29
2.4.4	Different types of PM motors	29
2.5	Switched Reluctance Motor Drives	31

2.5.1	Operation of SR motors	31
2.5.2	Torque production	31
2.5.3	Torque-Speed characteristics	32
2.6	Efficiency of electric motors	33
3	Efficiency Map Generator	37
3.1	Efficiency model	37
3.1.1	Model adapted to data	37
3.2	Data collection	39
3.2.1	Image reading	39
3.3	Creating efficiency maps	41
3.4	Example of usage	44
4	Electric Motor Performance Estimation Tool	49
4.1	Comparison of the electric motors	49
4.1.1	General considerations	50
4.1.2	DC motors	52
4.1.3	Induction motors	52
4.1.4	PM motors	53
4.1.5	SR motors	54
4.1.6	Motor property ratings	54
4.2	Motor type parameter selection	55
4.2.1	Efficiency scaling	55
4.2.2	DC motor	56
4.2.3	Induction motor	56
4.2.4	PM motor	57
4.2.5	SR motor	57
4.2.6	Motor model parameters validation	58
4.3	Generating VEM data	62
4.4	Simulations in VEM	63
5	Conclusions and future work	67
5.1	Conclusions	67
5.2	Future work	68
	Bibliography	69

Chapter 1

Introduction

In this chapter an introduction to the thesis work is given, including background, purpose, goals and the methods used.

1.1 Background

Vehicle Energy Model (VEM), is developed by LeanNova Engineering AB in Trollhättan for simulation of different vehicle configurations in MATLAB/Simulink. The model is designed to be able to follow predefined speed profiles or driver commands which brings the possibility of studying many different driving conditions. When designing an electric drivetrain, this model can be used to do initial studies of efficiency and performance. Correct component models and data are essential for validity of the results. Data of components is however not always available, but one way of obtaining this is to make estimations based on key metrics of known components such as electric motors.

1.2 Purpose and goals

When there is a lack of real measured data, a need arises for data that can be used as an estimation of the specific component properties. This work considers how to handle a lack of information regarding the performance of different electric motors. If this information is available it can be used together with VEM to compare different electric motor types for a given vehicle or application. The purpose of this work is to make this information available for use with VEM by investigating electric motors that are feasible for vehicle propulsion. The objective is to develop methods and an Electric motor Performance estimation Tool (EPT) that generates estimations of performance properties, like torque and efficiency data for the possible operating points for different types of electric motors. Data generated by EPT should be designed to fit the input interface of the VEM developed and used by LeanNova for simple integration with the existing system. How this is intended to work is illustrated in Figure 1.1, where we can see that the electric

motor characteristics estimated by the EPT is used as input in the motor plant of the VEM. Based on the current motor torque request, motor speed, battery voltage and power cut torque, the actual torque and output power of the motor are calculated.

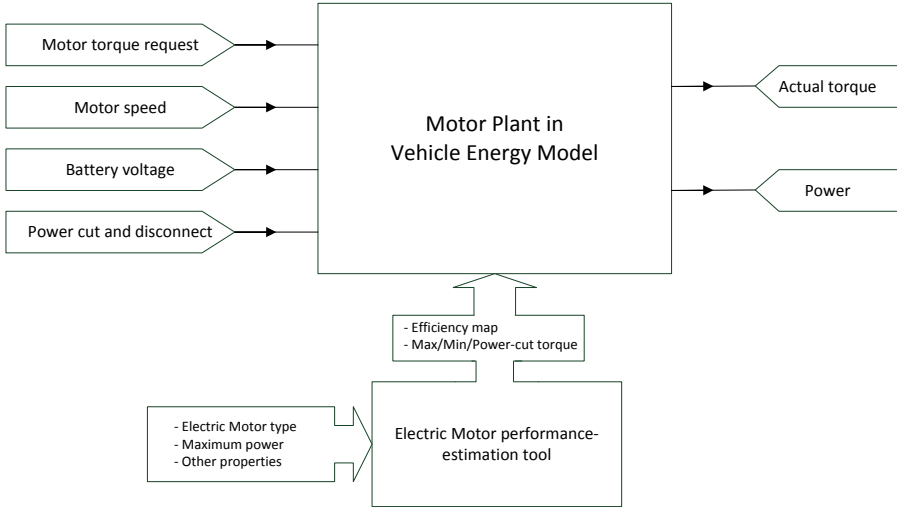


Figure 1.1. Overview of the EPT with input to the VEM.

1.3 Related research

There are a lot of special requirements for an electric motor to be feasible for a vehicle powertrain. This is a topic discussed in [1] and their classification of electric motors for electric vehicles (EV) can be seen in Figure 1.2.

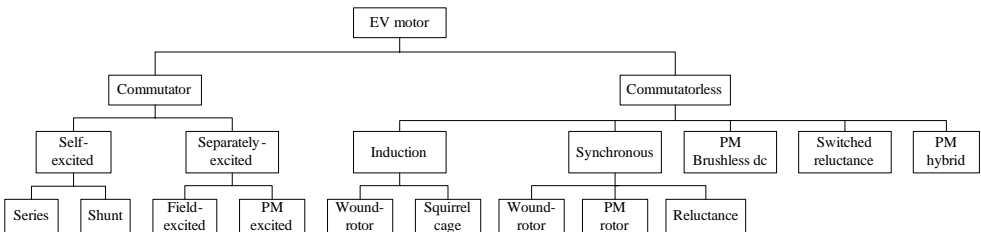


Figure 1.2. Classification of EV motors according to [1].

When comparing the discussions in [1] with other work done in this area the conclusion is that there are four main types of electric motors that are of interest when choosing motor for an EV. If the discussions in [1-6] are weighed together

the main categorization can be summarized as Direct Current (DC) brushed motors, Induction motors, Permanent Magnet (PM) motors and Switched Reluctance (SR) motors. According to [2] the traditionally used DC brushed motors are getting outclassed by the modern Induction and PM motors and therefore are of less interest today.

In [3] it is clearly displayed how the Induction and PM motors are the most widely used motors in vehicles produced the last years. It is explained in [4] that PM motors have higher power density than the Induction motor and therefore have a high potential for the future. The high potential of SR motors is also discussed but it is explained that they are still suffering from issues, described in Section 4.1.5, that needs to be solved before becoming a serious threat. Some work treating the difference between electric motor efficiency maps has been done earlier and in Figure 1.3 it is displayed how a typical efficiency map for some different motor types can look like.

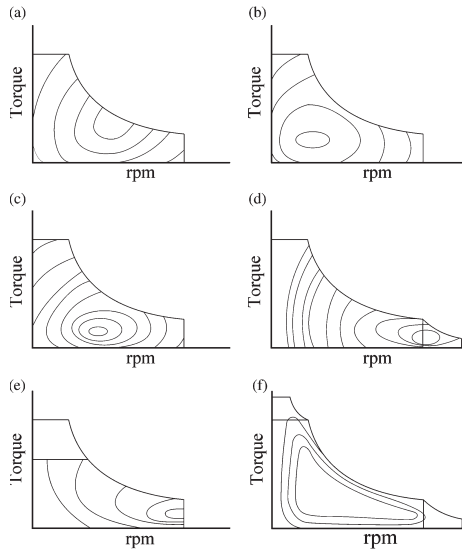


Figure 1.3. Efficiency maps for 6 different EV motor types according to [3]. An illustration of the idea with typical performance properties for different types of motors. We can see that the motors have different high-speed and high-torque capabilities. The efficiency is low close to zero torque or rpm.

1.4 Approach

When analyzing the EV motor types it is important to investigate how they differ in performance and other properties. During simulations of vehicles in VEM a difference in energy consumption can be detected between different configurations. This makes some properties more interesting than others when studying the EV

motors in this work. The following lists declares which properties that are of highest interest.

- Efficiency in different operating points
- Possible motor speed
- Maximum torque for a given speed
- Power density

There are also properties that is of less interest during the simulations in VEM but of big importance in practice. Some of these are listed below and are also taken into consideration to some degree.

- Dynamic performance
- Temperature and geometry dependencies
- Maintenance demands
- Sound level
- Production cost

The idea for how EPT is suppose to work is to determine the typical efficiency map and torque curve characteristics for each motor type, which then is scaled with respect to the desired maximum power. The differences in design and other properties of the motor types also makes the efficiency maps and torque curves different. The result should then be similar to what is displayed in Figure 1.3.

To be able to determine the typical properties there is a need of data about each motor type. Information about different motors can for example be found in literature, scientific reports, and data sheets from manufacturers. If motors and equipment is available, this information can also be obtained by measurements. During this work some data was available from start but most of the information used is collected from reports. Since almost all the efficiency map data, found is in the form of a contour image, another tool is developed to be used for data collection. This tool is named Efficiency Map Generator(EMG) and turned out to be very useful also outside this work.

For the understanding of collected data, and how it should be used in this work, it is important to investigate the underlying phenomenons. The electricity and magnetism that is the foundation for the electric motors is discussed in [5] and [6] and the different types of electric motors is then deeply investigated in [7]. With the help of this material and other concerning EV motor control like [1], [2] and [8], the goal is to determine the typical properties for each motor type and to understand the reasons behind their differences.

1.5 Thesis contributions

This thesis first brings a summary of the electric motors that are feasible for vehicle propulsion. It is made in a way to give someone without experience a quick background to understand why the motors are different when it comes to performance in vehicle propulsion applications where other factors are of importance compared to the traditional industrial use of electric motors. Extra focus is put on the understanding of the torque curve and efficiency map of the different motors since those are the properties of greatest interest in this work. A modification to an existing physical efficiency model for electric motors is presented to better capture the effects that high power operating has on the motor efficiency. The EMG describes methods for collecting motor data and how it can be combined with the physical efficiency map model to create good input data for simulations. The report also brings a summary of comparative studies of the different electric motor types regarding performance in vehicle propulsion. This consists of information useful during concept selection to when a decision has to be made regarding what motor type that shall be used in an application. The last contribution of this work is the proposed motor models in the EPT that are based on all the information collected in the previous parts of the work. The models are also presented together with a method of scaling the maximum efficiency of the motors depending on the motor size.

1.6 Outline

The thesis includes the following chapters:

Chapter 1, Introduction: Presents the work and its background together with the methods used and results.

Chapter 2, Electric Motors: Describes the basic electricity and magnetism behind electric motors. The chapter then presents the four different motor types based on this information and also how to model their efficiency.

Chapter 3, Efficiency Map Generator: The tool made for gathering information and creating input data is presented.

Chapter 4, Electric Motor Performance Estimation Tool: A comparative study of the electric motor types regarding vehicle propulsion is presented and how this information is used to create the motor models used in the EPT.

Chapter 5, Conclusions and future work: Conclusions of the work is presented and a discussion about future work.

Chapter 2

Electric Motors

The different types of electric motors can at first glance seem very dissimilar, but the physical principles of electricity and magnetism are something they all are using. This chapter presents the underlying basic phenomenons which is the foundation for the function of electric motors by studying the DC brushed and induction motors to some depth for getting the basics for understanding electric motor operation and also describes the fundamental principles of PM and SR motors.

2.1 Electricity and magnetism

When an electric motor is being used it is converting electrical energy to mechanical energy. It can also be used in the opposite direction as a generator, and in a vehicle both these operating modes are of importance. During conversion of energy between the electrical and mechanical domains a third domain is involved, namely the magnetic domain [7]. Magnetic fields and magnetic flux are therefore important factors for the understanding of electric motors.

2.1.1 Magnetic fields

There can be different sources for a magnetic field, the most common way to encounter and see the effects of a magnetic field is when managing magnets. In Figure 2.1 we can see a big permanent magnet with the magnetic field it produces drawn as lines with arrows in the direction of the magnetic flux Φ . Just like how the needle in a compass aligns with the magnetic field of the earth, the small magnets in Figure 2.1 aligns with the field of the big magnet. The force acting between the magnets can be seen as something similar to the gravitational force from earth. Potential energy can be stored by separating them by force and this energy is then released when releasing the magnets. This makes it easy to understand that a system consisting of only magnets can not be continuously moving, energy needs to be added or withdrawn in order to make something change.

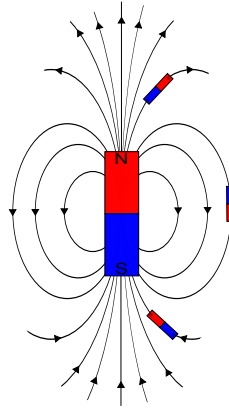


Figure 2.1. Magnet with the magnetic field drawn as field lines going from the north to the south pole.

2.1.2 Producing a magnetic field

In [6] it is described how a conductor carrying a current is related to a surrounding magnetic field. If there is a magnetic field close to a conductor, then a current is induced and a conductor that is fed with a current will induce a magnetic field, the directions of the current and the magnetic field with respect to each other is illustrated in Figure 2.2.

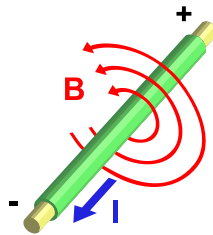


Figure 2.2. Conductor carrying a current I surrounded by a magnetic field with flux density B . (Source: <http://commons.wikimedia.org/wiki/File:Electromagnetism.svg>)

Different materials have different permeability, this is basically the willingness of the material to cause a magnetic flux when exposed to a magnetic field. Materials of high permeability can therefore be used together with electric currents to produce magnetic flux. By combination of the idea that electric currents produce magnetic fields and that some materials, like iron, have high permeability an electromagnet can be constructed. In Figure 2.3 an electromagnet is illustrated, it consists of an iron core with copper wire wound around it. When a current is flowing through the copper wire a magnetic field is induced very similar to that of the permanent magnet in Figure 2.1. The relationship between the directions of the current in a winding and the induced magnetic field can be described with

the *right-hand rule* in two equivalent ways [7]. The first way is described as if you grab a current carrying conductor with the right hand and the current is flowing in the direction of the thumb, then the magnetic field has the same direction as the other fingers according to Figure 2.2. Equivalently if a coil is grabbed and the fingers is pointing in the direction of the current, then the magnetic field has the same direction as the thumb as can be seen if grabbing the iron core in Figure 2.3.

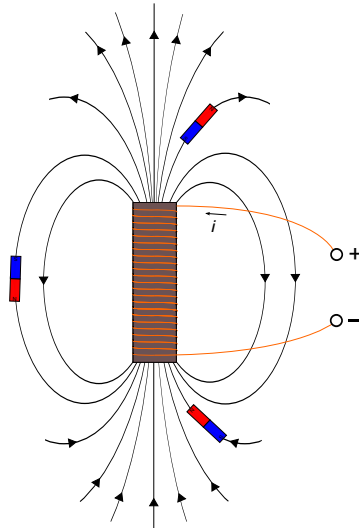


Figure 2.3. Iron core with copper winding carrying a current.

2.1.3 Magnetic flux density

It is easy to notice that a magnetic field varies in strength, when holding a magnetic material close to a magnet the force is much bigger than when holding it far away. This can also be illustrated by the lines in Figure 2.3, if we think that there is an equal amount of magnetic flux between a pair of lines when following them from one side to the other it is obvious that the density of the flux must be different. Close to the electromagnet the lines are very close together which would imply high density, as the force also is higher close to the electromagnet it is natural to think that the magnetic flux density B is closely related to the forces in magnetic fields. The magnetic flux density can be defined by

$$B = \frac{\Phi}{A}, \quad (2.1)$$

where A is the area through which the magnetic flux is flowing.

2.1.4 Force on a conductor

In [6] the *Lorentz's force equation* is explained in detail and how it tells us about the total electromagnetic force acting on a charge in both electric and magnetic fields. When a conductor of a length l is carrying a current I in a magnetic field with magnetic flux density B perpendicular to the current then the force acting on the conductor can be expressed as

$$F = BIl , \quad (2.2)$$

as we can see the force is proportional to all the mentioned parameters and this is one of the two principles used in electric motors for producing torque [4]. The direction of the force in relation to the field and current can also be illustrated by a *right-hand rule*, this is illustrated in Figure 2.4.

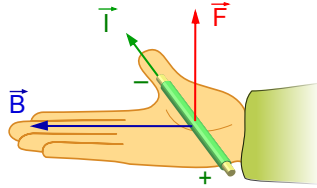


Figure 2.4. Direction of Lorentz force acting on a conductor. (Source: <http://en.wikipedia.org/wiki/Lorentzforce>)

2.1.5 Magnetic circuits

As the magnetic flux tends to pick the easiest way from one pole to the other its path can be confined by making circuits of materials with high permeability. In Figure 2.5 a magnetic circuit is made by a loop of iron with an air gap and a winding similar to that of the permanent magnet. We can now see that the magnetic flux still has to cross air to get from one pole to the other, but now it can follow a path with much lower "resistance". Since it is the conductor that is inducing the magnetic flux with contribution from every turn and the size of the current, it is reasonable to think that both the current i and the number of turns N could be proportional to the flux. This discussion brings up the idea of an analogy to the electric circuit. Electric circuits and how to make calculations based on their configuration is explained deeply in [5]. By introducing magnetomotive force (MMF) \mathcal{F} as the product of the current and number of turns in the winding, and reluctance \mathcal{R} as the earlier mentioned "resistance" in the circuit, the analogy can be seen by comparing the two expressions where the first one is ohms law for electric circuits [7]

$$I = \frac{V}{R} \quad , \quad \Phi = \frac{Ni}{\mathcal{R}} , \quad (2.3)$$

here we can see that the MMF match the voltage and that the magnetic flux just like the current in the electric circuit acts as a flow.

The reluctance in the magnetic circuit consists of different components just like the resistance in an electric circuit. If the magnetic circuit in Figure 2.5 is considered it is the reluctance of the air gap that is dominating and brings almost all reluctance to the circuit, since the reluctance of the iron core is much smaller it can be neglected. This is something that makes calculations much easier in many cases and when working with electric motors this is an acceptable action since they involve dominating air gaps.

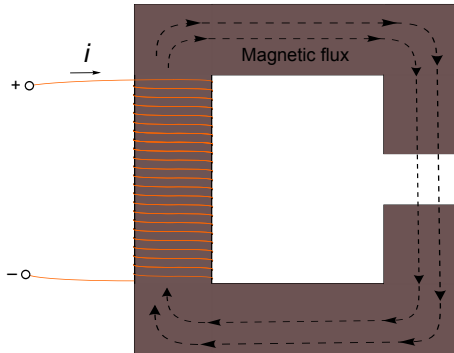


Figure 2.5. Magnetic circuit made of a iron core.

The reluctance of the air gap is defined by its geometry and also by the permeability of air. If the cross-sectional area of the air gap is A and its length is g the reluctance is defined by

$$\mathcal{R} = \frac{g}{\mu_0 A}, \quad (2.4)$$

where μ_0 is the permeability of air.

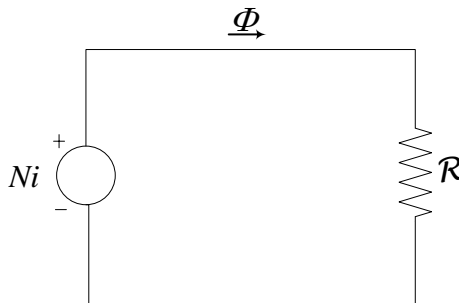


Figure 2.6. Equivalent circuit for the magnetic circuit in Figure 2.5.

As stated by (2.2) the magnetic flux density is important to generate torque in an electric motor. By combining (2.1), (2.3) and (2.4) the magnetic flux density can be calculated in a circuit as

$$B = \frac{\mu_0 N i}{g}, \quad (2.5)$$

it is thereby clear that a small air gap contributes to a high flux density required for producing a large force on a conductor.

2.1.6 Reluctance torque

The magnetic flux does not only seek the easiest way through a magnetic circuit. It also tries to make the reluctance smaller by exerting force on the circuit in ways to achieve this. In Figure 2.7 it is illustrated how a torque T is affecting an iron piece on a rotating axis situated in the air gap of a circuit. If the iron piece gets aligned with the magnetic field flowing through the circuit the cross-sectional area get as large as possible and thereby the reluctance as small as possible according to (2.4). This reluctance torque is the second principle for producing torque in electric motors and the only one used in SR motors [4]. If a winding would have been put on the rotating iron piece in Figure 2.7 there would have been torque produced both from the mutual interaction between the two fields and the changing reluctance thus both principles would have contributed.

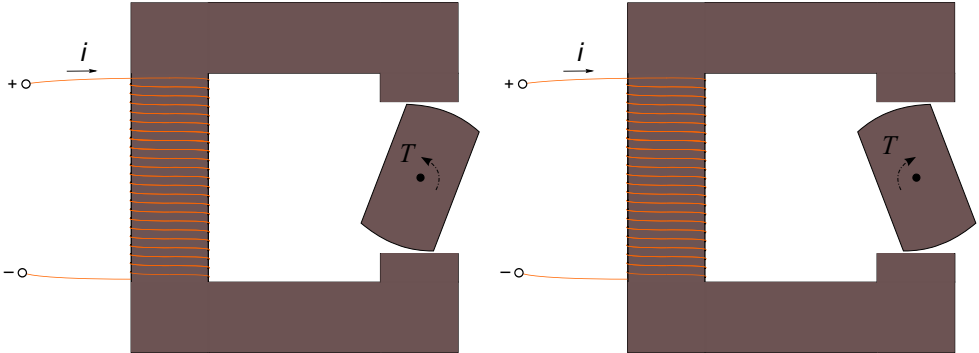


Figure 2.7. Magnetic circuit with a rotor inserted into the air gap. Notice that the torque has different direction depending on the rotor position.

2.2 DC Motor Drives

This section describes the simplest of all electric motors. The brushed DC motor has been popular for a long time because of the simple and cheap construction. The simplicity of controlling the motor is also an important factor for its success over the years.

2.2.1 Operation of the DC motor

In Figure 2.7 it can be seen how a magnetic field can make a piece of iron to a rotor. In that case it was affected by a force because the field worked in a way to minimize the reluctance. If the rotor had been cylindrical the reluctance would have been the same for every position around the rotating axis hence the torque in the wrong direction depending on position is removed. By making the rotor cylindrical and adding conductors close to the surface in slots and which carries currents along the rotor axis the torque from the *Lorentz's force* (2.2) can be used in an effective way. By putting the conductors in slots the force is also acting directly on the rotor and thereby saving the conductors from stress.

Since it is not entirely all the magnetic flux that stays in the iron core in an magnetic circuit there is also some losses in the form of leakage flux. One way of handling this is by positioning windings close to each other and also close to the location where a high flux density is desired. In Figure 2.8 a cross-section of a DC motor is displayed. We can see that the winding that is producing the magnetic field has been split up into two parts, one above and one below the rotor. The magnetic flux is then flowing through the rotor and around the circuit back to the top and down again, when it is passing the very small air gap it is also passing the current carrying conductors. When studying the direction of the magnetic field and the direction of the current in the conductors we can very easily use the *right-hand rule* to see that force will affect each conductor so that a torque will be put on the rotor in the direction marked in the figure.

Commutator

The commutation principle is the thing that is specific for brushed DC motors. This is also the issue which causes the negatives side of this motor type. As we can see in Figure 2.8 the conductors in the rotor has the perfect correct direction when they are close to the magnetic flux so that a force is applied in the direction on the conductor to make the rotor rotate in the desired rotational direction. In the upper part of the rotor the current is going into the page which causes a force to the left. In the lower part of the rotor the current is going out from the page which causes a force to the right. Between these sections there is conductors that is disconnected and not carrying a current because they are in a bad position and can not deliver any useful torque.

This change of direction of the current in the rotor is called commutation and it is done mechanically in the brushed DC motors. It is often done by using two

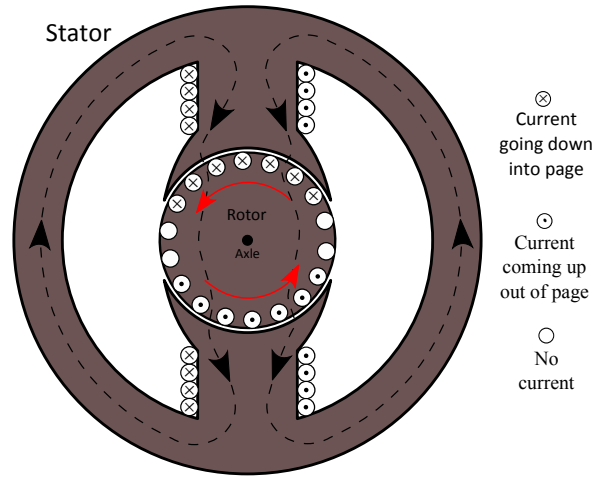


Figure 2.8. Cross-section through a DC motor with two poles, each pole corresponds to a winding, the path of the stator field as dashed lines. In this case the stator field is excited by a coil but it can also be supplied from a permanent magnet. The red arrows shows the direction of the torque applied on the rotor.

brushes of carbon that are pressed against the ends of the rotor windings while it rotates and thereby supplies them with current in one direction while they have contact on the first half of the lap and then the current change direction when the same wire ends come in contact with the other of the two brushes on the second half of the lap. By designing the brushes in the way we want we can get the configuration illustrated in Figure 2.8 and then the rotor always has force applied in the direction of rotation. The drawbacks with commutation is mainly because it is mechanical which means noisy operation and also wear of the brushes which results in a motor with a big need of maintenance.

2.2.2 Torque production

If studying one pair of conductors on the rotor which is on opposite sides of each other, they always have current in different directions thus they can belong to a coil wound around the rotor. If this coil has N turns, and if the radius of the rotor is r , then the maximum torque T provided to the rotor from this pair of conductors with the force (2.2) is given by

$$T = 2NrBIl, \quad (2.6)$$

since $2rl = \text{area of coil}$ this expression multiplied by B can be replaced with Φ which gives

$$T = N\Phi I, \quad (2.7)$$

which is the peak torque described by the flux through the coil. Since this is only the peak torque from one coil and does not consider the amount of poles in the

motor a constant can be introduced called the *winding constant* K_a [7], which gives a good description of the whole motor. With this constant the expression for the torque becomes

$$T = K_a \Phi I , \quad (2.8)$$

and it describes the torque from a general DC motor. The winding constant K_a depends on the design of the motor according to the following expression [7]

$$K_a = \frac{\text{poles } C_a}{2\pi m} , \quad (2.9)$$

where

poles = number of poles on the stator

C_a = total number of conductors in rotor winding

m = the number of parallel paths through the winding

The important conclusion drawn by studying (2.8) is that the torque produced is proportional to the current I in the rotor windings and the flux from the stator field Φ .

2.2.3 Electro Motoric Force

According to *Faraday's law* there is a voltage induced in a conductor travelling through a magnetic field described by

$$E_b = Blv , \quad (2.10)$$

where l is the length of the conductor and v is the speed with which it is travelling. If studying the same coil as in Section 2.2.2 when the rotor is rotating with the rotation speed ω then the speed of the conductors can be written as $v = r\omega$ and with the number of turns N and the fact that there is two conductors per turn gives the voltage

$$E_b = 2NrBl\omega , \quad (2.11)$$

and by comparing this with (2.6) it is likely that the expression also can be rewritten with the *winding constant* from [7] to become

$$E_b = K_a \Phi \omega , \quad (2.12)$$

which is just like (2.8) describes the general behaviour of the DC motor. E_b is named back Electro Motoric Force (EMF), and by studying (2.12) it is realized that this voltage induced in the motor is direct proportional to the rotor speed which is a very important property.

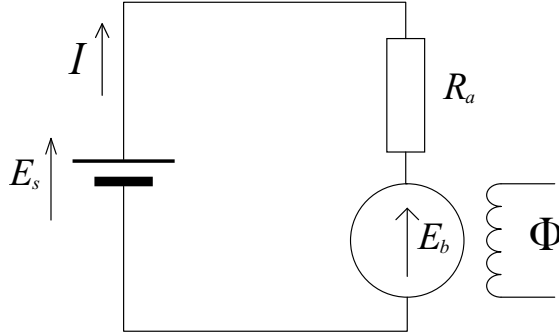


Figure 2.9. Static equivalent circuit for a DC motor with a magnetic field Φ provided from an undefined source.

2.2.4 Torque/Speed control

The DC motor can now be described as an equivalent circuit. If the resistance of the conductors in the rotor is denoted R_a and the voltage supplied to the rotor is E_s , the circuit can be drawn as in Figure 2.9.

From this circuit the following expression can be obtained by using *Kirchhoff's voltage law* as the current I is flowing through the rotor

$$E_s = E_b + IR_a, \quad (2.13)$$

if rewriting the expression in a way to obtain the current I and by substituting E_b with (2.12) the expression is transformed to

$$I = \frac{E_s}{R_a} - \frac{K_a \Phi}{R_a} \omega, \quad (2.14)$$

and finally by substitution with (2.8) the relationship between torque and rotational speed can be obtained as

$$T = \frac{K_a \Phi E_s}{R_a} - \frac{(K_a \Phi)^2}{R_a} \omega. \quad (2.15)$$

This equation is important and displays very clearly how the DC motor can be controlled and also what behaviour that should be expected from the motor. Since the second term is negative we can see that the DC motor delivers the maximum torque at zero rotational speed. It is also clear that if all the parameters like voltage and fields are constant, the available torque declines linearly with the increase of speed and the maximum speed is reached when the torque has reached zero and no more acceleration is possible.

By studying Figure 2.10 it can be seen that the supply voltage E_s only affects the constant term. This means that the torque-speed curve can be adjusted vertically by adjusting the supply voltage. Since the torque is proportional to the

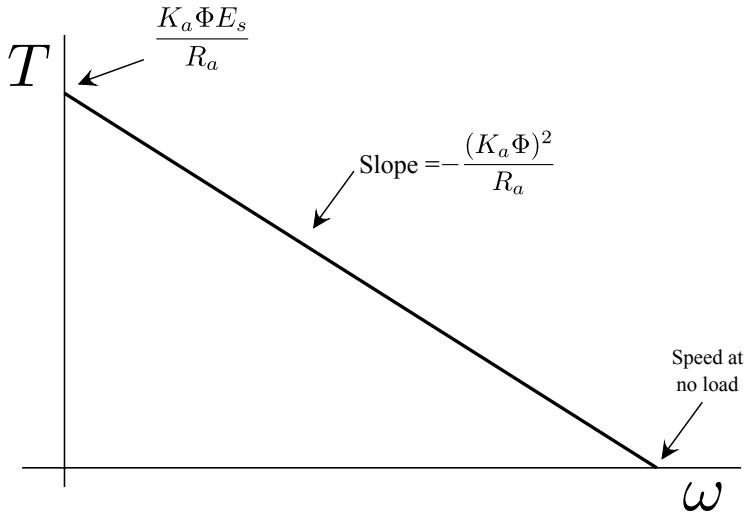


Figure 2.10. Torque-speed characteristics for constant source voltage E_s and field strength Φ .

current and there is a limit in maximum current for the protection of electronic equipment it is also a maximum possible torque, there is also a maximum power that can be delivered for every device. By adjusting the supply voltage the desired speed can be achieved for every torque below maximum torque and as long as the output power is below maximum. This way of controlling the motor is called armature control [1]. We can also see that the field strength is affecting both the constant term and the slope of the curve. This means that if it is possible to weaken the field the slope can be flatter and the maximum torque is decreased, but this also would mean that higher speed operation is possible. This way of controlling the motor is called field control [1] and is only possible if the field is excited by a source that can be controlled, thus not on motors with permanent magnet stator. In Figure 2.11 it is illustrated how the motor can be controlled in the possible operation point area with both armature and field control.

If the field is excited by a coil it can be connected in three classic ways. The field coil can be connected in series or parallel (shunt) with the the source powering the rotor and it can also be powered by a separate field voltage source denoted E_f . The big advantage of a separately excited motor is that it allows independent control of the magnetic flux Φ (by varying E_f) and the supply voltage E_s , which makes it easy to use all the possible operating points as in Figure 2.11. The field coil is then of the same principle as the magnetic circuit in Figure 2.5 and the relationship between E_f and Φ can be described with the equations (2.3) and (2.4). When the need of extensive controllability is less prioritized than the cost, the permanent magnet stator configuration can be an attractive choice.

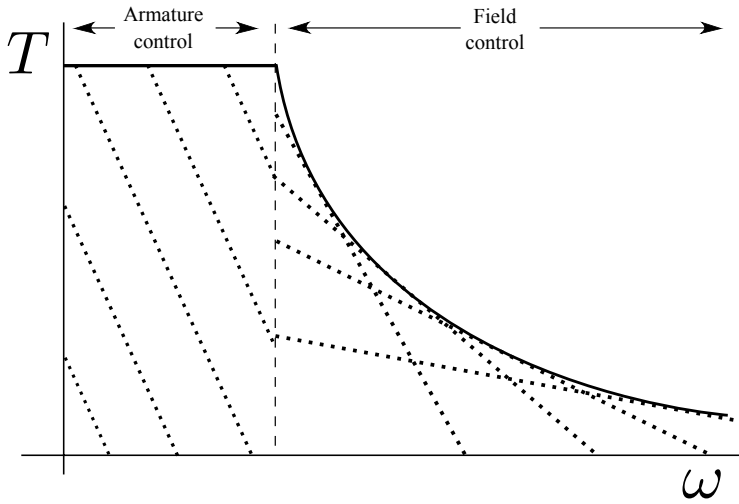


Figure 2.11. Illustration of armature and field control for DC motor with varied torque-speed characteristics (dotted lines). During armature control the slope of the torque-speed curve is constant since E_s is varied, when using field control the slope is different since Φ is varied. The possible operation point area is limited by the maximum torque (current) and maximum power. A maximum speed limit is then added to protect the motor from mechanical damage.

2.3 Induction Motor Drives

In this section the induction motor is discussed. It is one of the most popular electric motors for vehicle propulsion today and still it has a long history. First some new things is going to be introduced that is essential for the understanding of induction motors since the way it is operating is a bit more complex than that of the earlier discussed DC motor.

2.3.1 Alternating current

The main difference from the DC motor is that the induction motor is powered by alternating current instead of direct current. This means that the current is changing direction with respect to time. The most usual form of alternating current is in the form of a sine wave, the AC voltage $v(t)$ can then be described as

$$v(t) = \hat{V} \sin(2\pi ft) = \hat{V} \sin(\omega t) \quad (2.16)$$

where \hat{V} is the peak voltage, f is the frequency, ω is the angular frequency and t is the time in seconds. In Figure 2.12 the difference between the DC voltage and the AC voltage is illustrated. While the DC voltage is constant over time the AC voltage is continuously changing in the way of a sine wave described by 2.16.

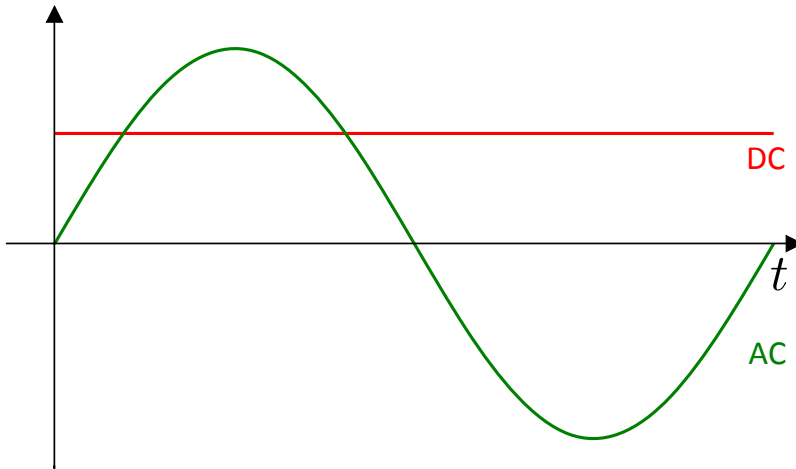


Figure 2.12. Alternating current compared to direct current.

2.3.2 The transformer

If we replace the air gap in Figure 2.5 with a second winding we get a transformer illustrated in Figure 2.13. Since the magnetic flux is following the iron core we now get two windings that both are related to the magnetic flux Φ in the core. By

using (2.3) we get the following relation between the currents in the two windings

$$\frac{N_1 i_1}{\mathcal{R}} = \Phi = \frac{N_2 i_2}{\mathcal{R}} \implies N_1 i_1 = N_2 i_2, \quad (2.17)$$

and we can say that the current and voltage are induced in the load side of the transformer from the source side hence power is transferred by *Induction*.

Ideal transformer

If it is an ideal transformer with no losses, the input power P_{in} must be the same as the output power P_{out} . Hence we also get the following relation between voltage and currents connected to the transformer

$$P_{in,out} = v_1 i_1 = v_2 i_2. \quad (2.18)$$

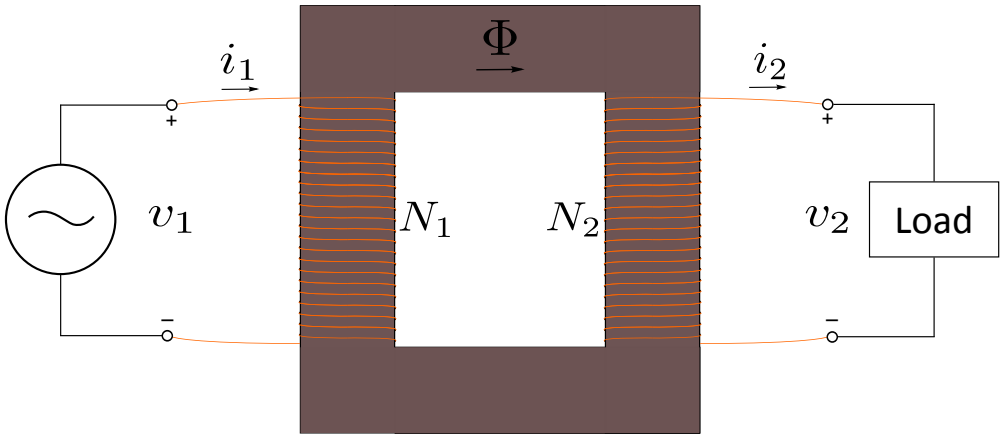


Figure 2.13. Ideal transformer connected to a voltage source and a load.

By combining (2.17) and (2.18) we can see that both the voltage and current is transformed when going from one side to the other according to

$$v_2 = \frac{N_2}{N_1} v_1, \quad i_2 = \frac{N_1}{N_2} i_1, \quad (2.19)$$

it is then clear that the ratio between the windings decides how the ratio between input-output voltage and current is going to be, and as the power is unchanged a lower current results in a higher voltage.

Equivalent circuit

By using the peak values from (2.16) a transformer with alternating currents can be described as an equivalent circuit as in Figure 2.14 (a) [7], there we can see

that the windings are replaced with the symbol for inductors. That is because they both have inductance which becomes an important property when working with alternating currents. We can also see that the load can be presented as an impedance Z_2 [5]. By studying the load side of the circuit we can see that

$$Z_2 = \frac{\hat{V}_2}{\hat{I}_2} \tag{2.20}$$

and by eliminating \hat{I}_2 and \hat{V}_2 with the use of (2.19), we get

$$Z_2 = \frac{\frac{N_2}{N_1} \hat{V}_1}{\frac{N_1}{N_2} \hat{I}_1} \implies \frac{\hat{V}_1}{\hat{I}_1} = Z_2 \left(\frac{N_1}{N_2}\right)^2 = Z'_2 \tag{2.21}$$

and that makes it possible for the circuit to be illustrated as in Figure 2.14 (b) with a new load Z'_2 that is Z_2 multiplied with the the square of the winding ratio. This means that Z'_2 is how Z_2 is perceived by the source, and it is said that the impedance is "referred" to the primary side.

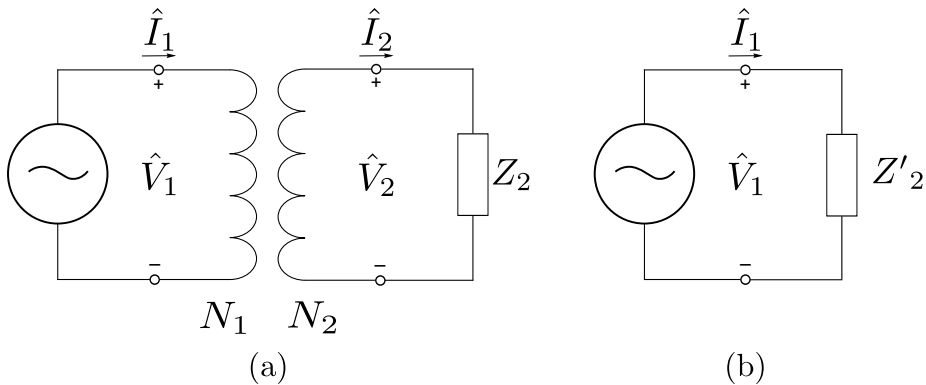


Figure 2.14. Equivalent circuit for an ideal transformer as in Figure 2.13.

The real transformer

The ideal transformer was studied for easier understanding of the referring principle. To get a good model of the real transformer all the losses and other neglected properties must be introduced in the circuit. As there is resistance in the windings of the transformer it can be introduced to the circuit as R_1 and R_2 in series with the source and load on each side. Even though almost all the magnetic flux flows inside the iron core and passes through both windings there is still some flux that does not follow this path and thereby disappears as losses. Since it is leaking from the path it is called leakage losses and it can be represented as leakage reactances X_{l1} and X_{l2} also in series with R_1 and R_2 . The third type of losses in a transformer is the iron losses from the magnetization also knowns as core losses.

These can be modeled as a combination between a magnetizing reactance X_M and a core loss resistance R_c [7]. If we use the relation between the current and the referred current in an ideal transformer from (2.19) we get

$$\hat{I}'_2 = \frac{N_2}{N_1} \hat{I}_2 \quad (2.22)$$

and then the equivalent circuit of a real transformer can be drawn as in Figure 2.15.

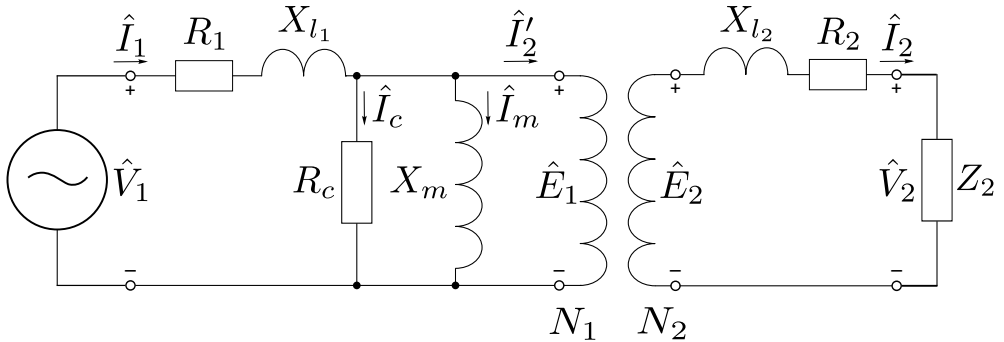


Figure 2.15. Transformer with losses introduced in the circuit.

By studying Figure 2.15 we can see that the middle part is an ideal transformer just like the one in Figure 2.14, so by using the referring principle in the same way we get a circuit as in Figure 2.16 where the real transformer is described in one single circuit with all the losses included.

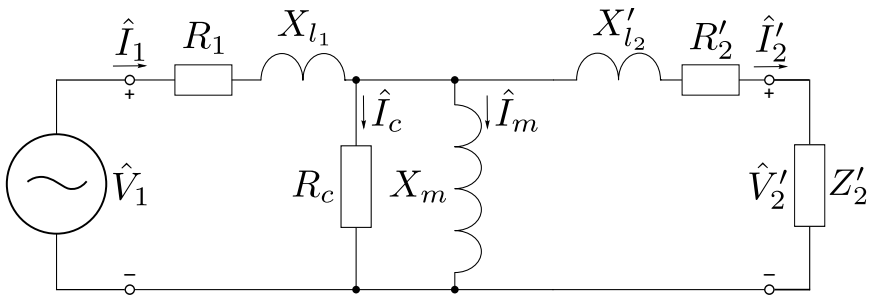


Figure 2.16. Transformer with losses introduced in the circuit after referring everything to one side.

2.3.3 Operation of Induction motor

If applying alternating current to a stator like the one described in Section 2.2 the field that is induced will be changing direction just like the current is changing since the relation is (2.3). In the DC motors the current direction is switched

by using a commutator which brings a lot of problems because of the friction that it brings to the system. By using alternating current this problem can be removed and thereby get reliable electric motors with low maintenance needs.

Three phase stator

Most induction motors used for vehicle propulsion is powered by three phase electric power which is a system where three different alternating current wires with different phases are combined. To get an even distribution the phase difference of the currents is $360^\circ/3 = 120^\circ$. This makes it possible to describe the currents in a three phase system as

$$\begin{aligned}
 i_a &= \hat{I}\cos(\omega t) \\
 i_b &= \hat{I}\cos(\omega t - 120^\circ) \\
 i_c &= \hat{I}\cos(\omega t - 240^\circ)
 \end{aligned}
 \tag{2.23}$$

if these three phases is combined in a stator with one coil each we get the appearance of Figure 2.17, where we can see that it results in a field that is rotating with the same frequency as the currents.

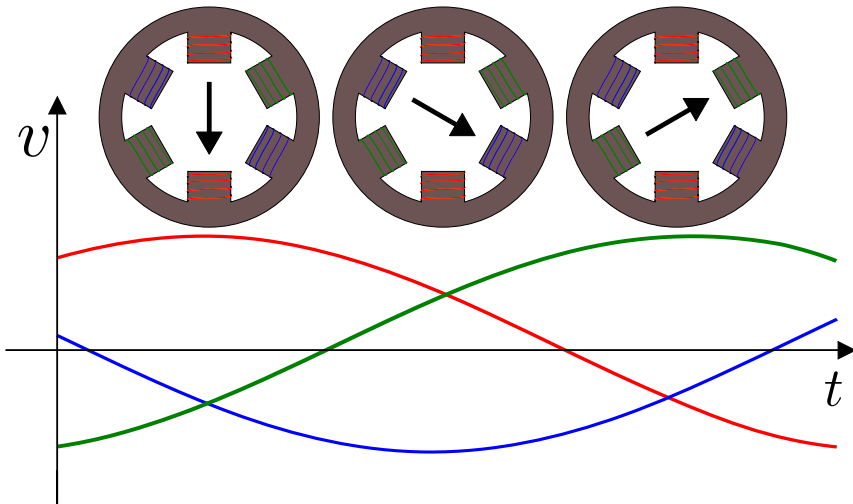


Figure 2.17. Rotating field as a result of 3-phase AC in a stator . The resulting direction of the field is approximately a sum of the field provided separately by the three different coils. This figure is a way to illustrate the rotating field, in reality the stator is cylindrical.

Squirrel cage rotor

When a stator with a rotating field is available as in Figure 2.17 there is just a need for a suitable rotor to get a complete electric motor. The most common rotors

for induction motors in electric vehicles is the squirrel cage rotors illustrated in Figure 2.18, this is basically a squirrel cage made of an inductive material. We can see that if we replace the arrows in Figure 2.17 with this squirrel cage as a rotor we would get a field B in the direction given by the blue arrow straight through the cage. According to (2.10) a conductor traveling through a magnetic field will have an induced voltage which if possible results in a current. If a squirrel cage is situated in the stator when the three phase voltage is applied, it will have a relative speed to the field and thereby a voltage will be induced. Since the squirrel cage is a circuit, a current can start flowing and as described by (2.2) a force will then be acting on the current conductor.

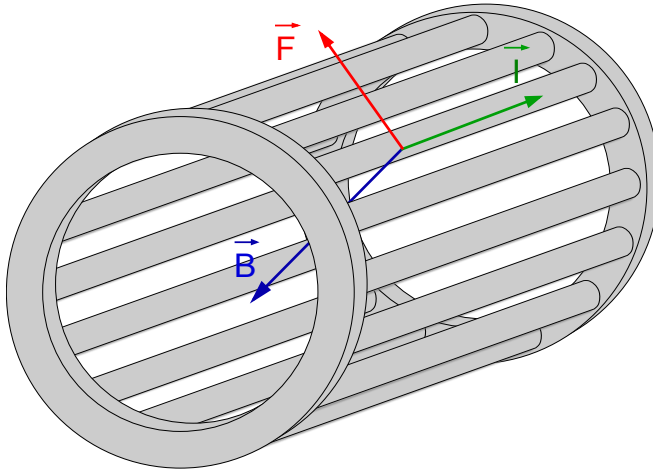


Figure 2.18. Squirrel cage that acts as the rotor in induction motors. Arrows for current, field and the resulting force are taken from the right-hand rule illustrated in Figure 2.4.

Slip

If the squirrel cage is put on a rotating axle inside the stator it becomes a rotor and the resulting force will make it start rotating. This means that the relative speed between the rotor and the rotating field will change. Since the force on the rotor is depending on the difference in speed, a result is that the rotor can not be affected by any force when it is rotating at the same speed as the field, which is called the synchronous speed. The difference in speed between the field and the rotor is usually expressed with the fractional slip s , which is calculated as

$$s = \frac{\omega_s - \omega_m}{\omega_s}, \quad (2.24)$$

where ω_s is the speed of the field and ω_m is the angular velocity of the rotor [7]. This means that when the rotor is at standstill the slip is 1 or 100% and if there is no load on the rotor it can almost get to the synchronous speed and thereby the slip is close to 0.

2.3.4 Equivalent circuit

Since the induction motor is transferring power between the stator and rotor by induction just like the transformer transfers power from one side to the other they can be treated in the same way. This is used when making a model of the induction motor as an equivalent circuit. The per phase stator side of the induction motor which is basically a winding delivering a magnetic flux just like the primary side of the transformer hence the equivalent circuit is identical. The difference between the transformer and the induction motor is mainly the varying speed difference between the stator and rotor which makes the frequency induced in the rotor also to become varying. By using the model of the transformer in Figure 2.16 and including the effect of the slip s , we get the single phase equivalent circuit for the induction motor in Figure 2.19 as it is explained in [7].

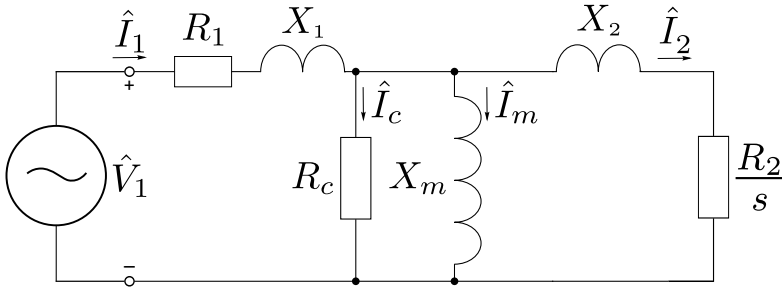


Figure 2.19. Equivalent circuit of induction motor.

Thevenins theorem

For making the analysis of the induction motor easier the Thevenins theorem can be used to simplify the circuit. This is done by introducing some new variables which depends on the variables seen in Figure 2.19 and the equations describing these variables are

$$\hat{V}_{1,eq} = \hat{V}_1 \frac{jX_m}{R_1 + j(X_1 + X_m)} \quad (2.25)$$

$$Z_{1,eq} = \frac{jX_m(R_1 + jX_1)}{R_1 + j(X_1 + X_m)} = R_{1,eq} + jX_{1,eq} \quad (2.26)$$

and with these equations the equivalent circuit can be described as in Figure 2.20.

2.3.5 Torque-Speed characteristics

This way of modelling the induction motor also makes it possible to express the produced torque T_{mech} as a function of the slip s as

$$T_{mech} = \frac{1}{\omega_s} \left[\frac{n_{ph} V_{1,eq}^2 (R_2/s)}{(R_{1,eq} + (R_2/s))^2 + (X_{1,eq} + X_2)^2} \right] \quad (2.27)$$

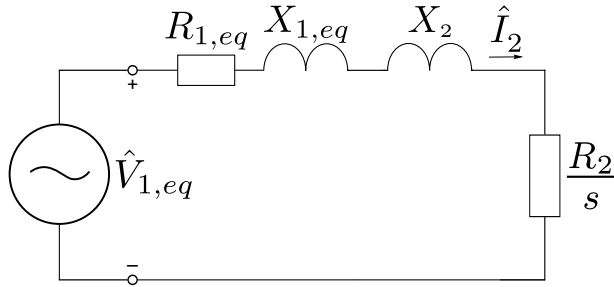


Figure 2.20. Equivalent circuit of induction motor simplified with Thevenin's theorem.

where ω_s is the speed of the rotating field and n_{ph} is the number of phases in the motor [7]. If we know the number of poles in the motor and the frequency of the supplied power f_e the synchronous speed ω_s can be described as

$$\omega_s = \frac{4\pi f_e}{poles} = \left(\frac{2}{poles} \right) \omega_e \quad (2.28)$$

where ω_e is the angular speed of the supplied electrical power. Since we are interested in the torque-speed characteristics of the motor we can get the torque T_{mech} as a function of rotor speed ω_m by inserting (2.24) into (2.27). If it is then plotted graphically the torque-speed characteristics of the induction motor can be illustrated as in Figure 2.21.

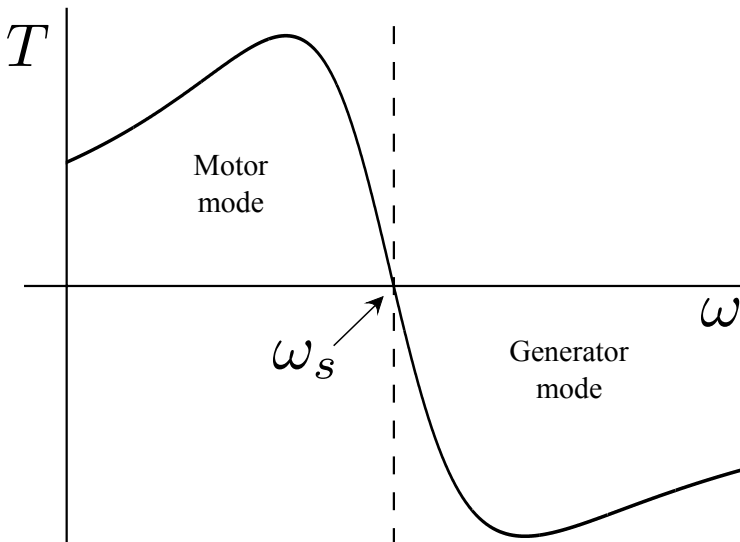


Figure 2.21. Torque-speed characteristics for induction motor. When the rotor speed is higher than the synchronous speed there will be a negative torque and the motor then acts as a generator.

2.3.6 Variable frequency control

Traditionally the induction motors have been very popular in constant speed operation because of the simplicity of the design which makes it cheap to produce and also because of the low maintenance needs that comes with brush-less operation. Recently they have also become a serious alternative when it comes to vehicle propulsion because good methods for controlling the speed have been developed. Currently most popular method used in this area is the variable frequency control. The idea of variable frequency control is to change the frequency of the power supply f_e and thereby move the synchronous speed ω_s along the speed axis of Figure 2.21, which makes the torque-speed characteristics change and the desired speed can be obtained for a specified torque. In Figure 2.22 it is illustrated how all the possible operating points in the motor mode can be achieved by varying the power supply frequency f_{e1-8} .

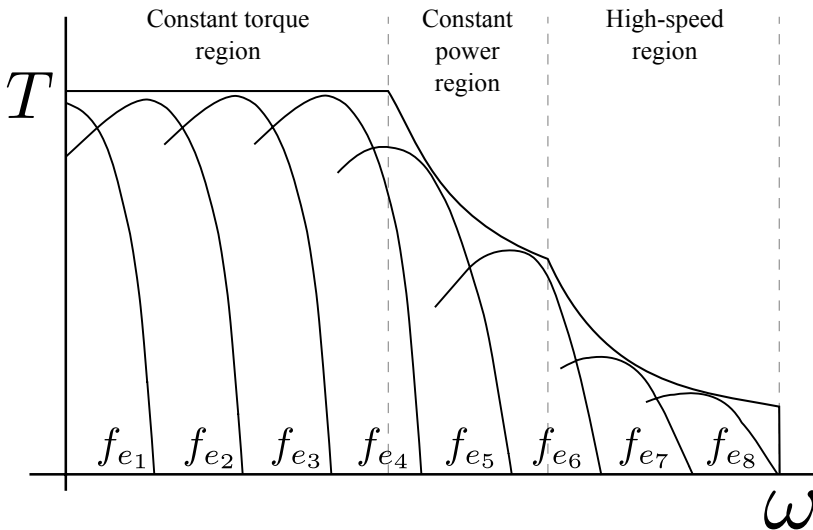


Figure 2.22. Maximum torque and speed curve for induction motor obtained with variable frequency control.

In Figure 2.22 it can be seen that the induction motor has three different operating regions in the motor mode. The constant torque region comes from the limitation in current that is necessary to protect the electric devices in the system. When the maximum power of the system is reached the motor enters the constant power region which is very similar with the one discussed in Section 2.2.4 for DC motors. Even higher speeds can be achieved with the loss of constant power by entering the high-speed region discussed further in [9]. The reason for this is that at very high frequency the deliverable torque is limited before the power supply has reached the power limit. When creating models in this work the high-speed region is approximated as a part of the constant power region.

2.4 Permanent Magnet Motor Drives

The permanent magnet motors are today the most popular motors for vehicle propulsion. This is mainly due to their high efficiency and high power density. But there are also drawbacks with this motor type, the use of rare earth metals in the permanent magnets is one of the drawbacks compared to other motor types.

2.4.1 Operation of PM motors

The stator of a PM motor can be described in the same way as for the induction motor. If we take the rotating field in Figure 2.17 and replace the arrow with a permanent magnet we will get Figure 2.23. Instead for a squirrel cage as rotor there is now a permanent magnet which follows the field and thereby rotates synchronously with the same frequency as the supplied voltage.

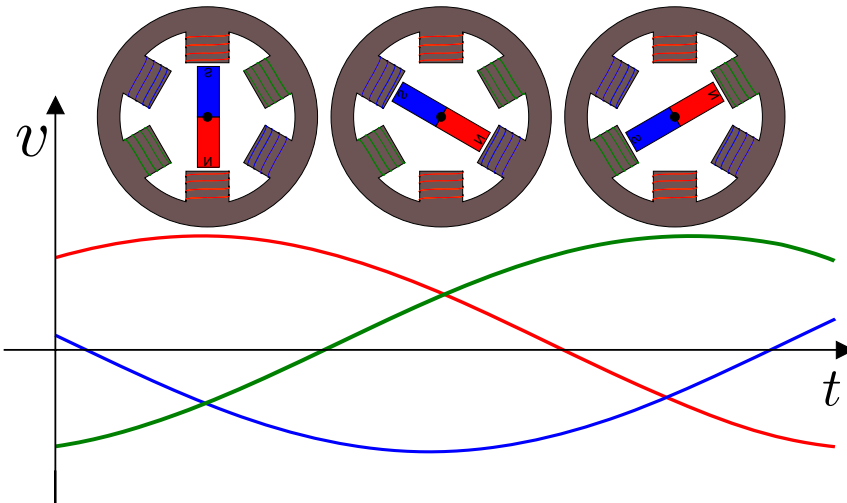


Figure 2.23. PM motor concept. The permanent magnet is rotating with the magnetic field.

2.4.2 Torque production

Since the permanent magnet wants to be aligned with the magnetic field there will be a torque applied to the magnet if it is not aligned. This means that the amount of torque the motor produces is depending on the angle between the magnetic field from the rotor and the stator called torque angle δ_{RF} [7]. In Figure 2.17 with Figure 2.23 we can see that $\delta_{RF} = 0$ in all three cases since the magnet has the same orientation as the field. In Figure 2.24 we can see how the delivered torque is a function of the torque angle. This means that the rotor need to have the same speed as the magnetic field for a constant torque to be produced. If the field would have a higher speed than the rotor or vice versa the torque would

change continuously since the angle is changing continuously and the mean of the torque would thereby become zero. Hence, the PM motor can not self start by a constant frequency source. In vehicle applications where the speed also needs to be varied this is solved by using variable frequency control, the same as described for induction motors in Section 2.3.6. By varying the frequency the speed of the PM motor can be controlled exact since it is always synchronous to the supplied frequency.

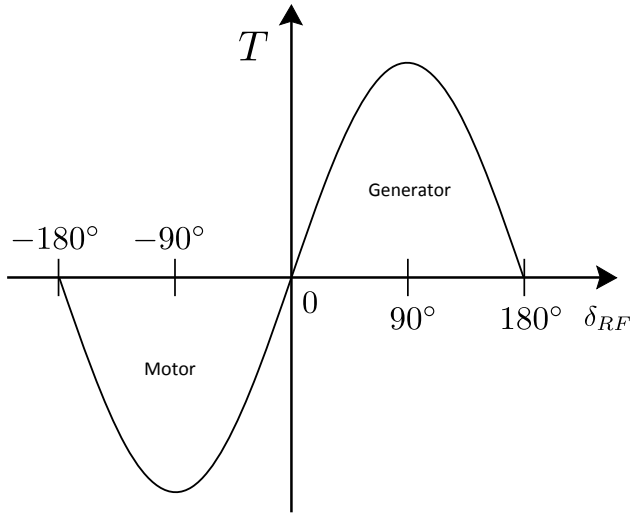


Figure 2.24. Torque as a function of the torque angle for PM motors.

2.4.3 Torque-Speed characteristics

The PM motors maximum torque-speed characteristics is quite the same as for the induction motors in but without the high-speed region, see Figure 2.22. So it is basically a constant torque region and then a quite short constant power region. This because the permanent magnet in the motor delivers a constant magnetic field, and thus the field weakening control which gives high speed is limited. A solution to this problem is to add windings and a control method to oppose the field from the magnet and thereby achieve higher speed operation. This type of motors is often refereed to as PM-hybrid motors.

2.4.4 Different types of PM motors

There are many different types of PM motors and they all share the good properties that the use of permanent magnets bring. One motor type that is included in this category is also the Brushless DC (BLDC) motor. This is because it has the same construction as described in this section, but it is fed from inverters that produce rectangular current waveforms instead of sinusoidal and hence the term

DC is used. The switching of the different DC voltages are then being initiated by rotor position sensors and thereby allows the motor to produce smooth torque [9]. The PM motors can also be designed in many different ways regarding both rotor and magnet placing. There can be both outer rotor and inner rotor PM motors which mean that the permanent magnets is outside and rotate around the stator windings. When it is the inner rotor type the permanent magnets is inside the stator winding on the rotating rotor, some different types of inner rotor PM motors can be seen in Figure 2.25. The cheapest way of creating the inner rotor is to make the magnets surface mounted which can be seen in Figure 2.25 (a) but it also creates more noise and windage losses than the other types where the magnets are hidden inside the rotor, Figures 2.25 (a)-(d).

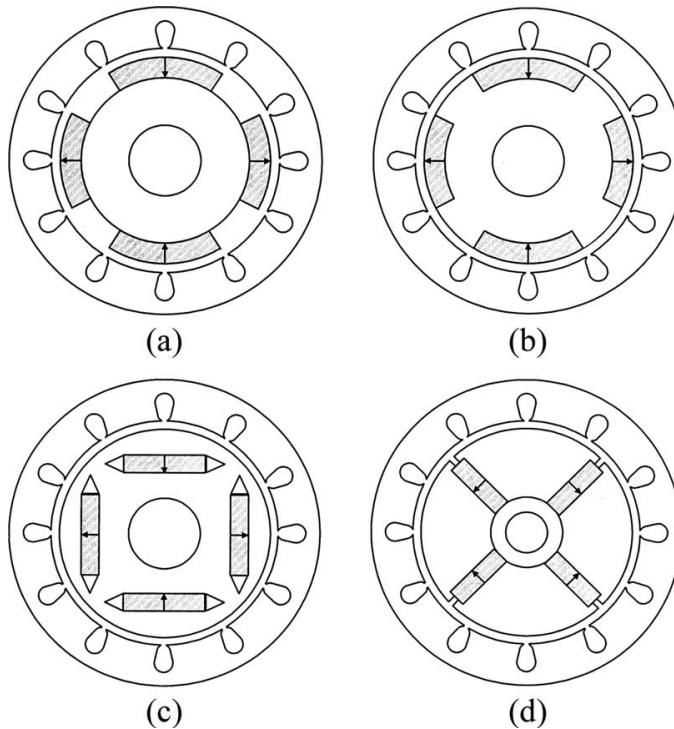


Figure 2.25. Different rotor PM motors displayed in [10]. (a) Surface mounted. (b) Surface inset. (c) Interior radial. (d) Interior circumferential.

2.5 Switched Reluctance Motor Drives

The switched reluctance motors can be seen as the dark horse in the competition between the different electric motors for vehicle propulsion. It has a lot of interesting properties that makes it to a very good candidate but still it has not become a popular choice. Some authors, e.g. [11], even states that the SR motors are ideally suitable for vehicle applications.

2.5.1 Operation of SR motors

The construction of the SR motors is simple. The stator is of the same kind as for induction and PM motors, but the rotor is made of solid iron which makes it very robust and cheap. In Figure 2.26 we can see how the SR motor is designed and how it is fed with a different voltage than in the PM and induction motor case.

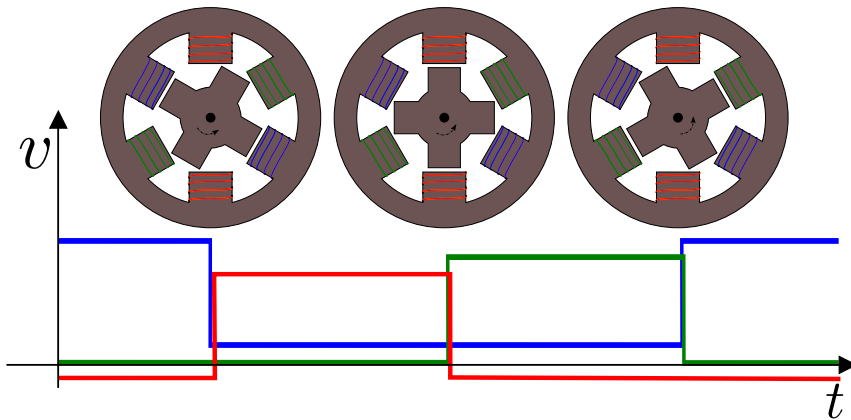


Figure 2.26. SR motor concept. The motor is used together with a conventional excitation technique [12]. In this figure the different phase voltages are displayed with a vertical displacement to make it clear that they belong to different phases for the reader who can not see the different colors. In reality the level and amplitude of all three phases are the same.

2.5.2 Torque production

The torque in the SR motor is produced using only the reluctance torque described in Section 2.1.6. The difference between the design in Figure 2.7 and the one in Figure 2.26 is that there are several windings in the latter. Voltage is applied to the different windings one by one to keep the rotor rotating. Once the rotor is aligned and the reluctance is minimized the power for that winding is switched off and the next winding is switched on. The inertia of the rotor keeps the rotor rotating during the switch between two windings. Since the torque is low when the rotor is aligned and the switch occurs there can be problems with torque ripple in this motor type. The torque ripple can be reduced in many different ways and

thereby make the motor more attractive. One way is to increase the number of windings on the stator and thereby the number of phases. This makes the next phase switch on before the first phase switch off, which prevents the torque from being zero at any time. In Figure 2.27 we can see the reason behind the torque ripple and also how it also can be lowered by lowering the maximum current for each phase, the total torque will be less but also the ripple.

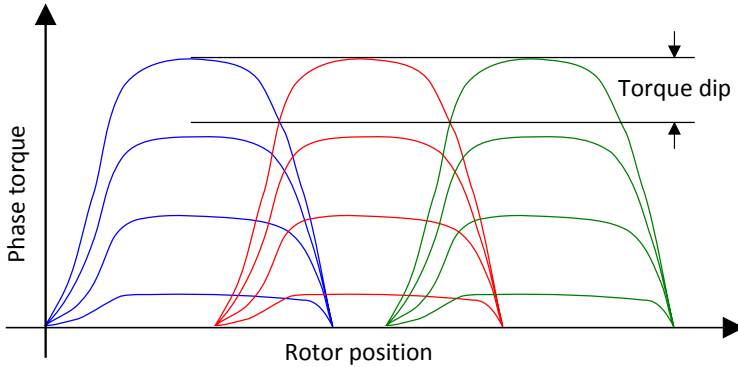


Figure 2.27. Torque-angle characteristics for an SR motor with four different current levels to illustrate how torque ripple can be reduced with lower current. The torque dip is an indirect measure of torque ripple since the total torque will be the sum of the torque from all phases, this is explained further in [4].

2.5.3 Torque-Speed characteristics

The torque-speed characteristics of the SR motors is similar to the induction motors in Figure 2.22 as it consists of three regions. There are both the constant torque region, the constant power region and a high-speed region. In the latter where the highest speed is achieved the product of the power and speed is constant which makes the torque decline rapidly when the speed gets higher. This region is usually a very small part compared to the maximum power region which can be wide for the SR motors and contribute to extremely high maximum speeds [4].

2.6 Efficiency of electric motors

When running an electric motor there is always different kind of energy losses. These losses are of big interest in vehicle applications since they affect the range of the vehicle. This section describes how the efficiency can be modelled for a DC brushed motor, but the result is also valid for the other motor types [8].

Copper losses

One of the biggest losses in all motors is the copper losses, this is the heat developed in the copper windings of the rotor. By multiplying (2.3) with the current I the power of the losses P_c in the rotor resistance R_a can be described as

$$P_c = I^2 R_a, \quad (2.29)$$

and by inserting (2.8) to eliminate I we get the following expression

$$P_c = \frac{R_a}{(K_a \Phi)^2} T^2 = k_c T^2, \quad (2.30)$$

where we see that the copper losses are proportional to the square of the torque and also inversely proportional to the square of the field. If the field is constant the constant k_c can be introduced and we get an expression of how the losses depend on torque [8].

Iron losses

Since the rotor is rotating in the field delivered by the stator, the iron in the rotor is exposed to a field that is changing direction in a frequency related to the rotor speed, resulting in two kind of losses.

The first one is the hysteresis loss, meaning that when the iron is magnetized by a field and then demagnetized by a field in the other direction there will be friction losses from aligning and realigning the magnetic dipoles in the material. In [7] the hysteresis loss power P_h is described as

$$P_h = K_h f B_{max}^n, \quad (2.31)$$

where f is the frequency with which the field changes direction, K_h is a proportionality constant depending on the iron properties, B_{max} is the maximum flux density and the exponent $n \approx 2.0$ for electric machines.

The second type of iron loss is due to electric currents induced in the iron when the magnetic field is passing through it. These currents are called "eddy currents" and they cause losses by producing heat in the iron because of the resistance in the material. By dividing the iron into sheets (laminations) which are isolated from each other these currents can be significantly reduced and the losses also becomes much smaller, this method is illustrated in Figure 2.28. In [7] the eddy current losses P_e are described as

$$P_e = K_e (B_{max} f \delta)^2, \quad (2.32)$$

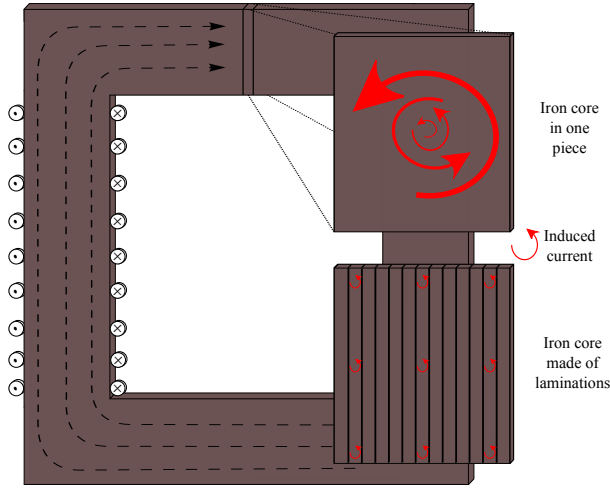


Figure 2.28. Illustration of how laminated iron cores reduce eddy currents.

where K_e is a proportionality constant and δ is the thickness of the laminations in the iron. Since both P_h and P_e are dependant on the frequency it is proposed in [8] to introduce a constant k_i which makes the iron losses proportional to the motor speed. This will in fact not really be constant as the value will be affected by the magnetic field strength and other non-constant factors. But usually a value can be found that gives a good indication of the losses, then we can describe them as

$$P_h + P_e \approx k_i \omega. \quad (2.33)$$

Friction and windage losses

As in all machinery there will be friction in the electric motor. Since there is only one rotating part all of the friction can be derived from the rotor bearings and commutator brushes which applies an approximately constant resistive torque T_f to the rotor. By multiplying T_f with the rotational speed the friction power losses P_f are given as

$$P_f = T_f \omega, \quad (2.34)$$

there will also be windage losses which is the air resistance applied to the rotor when rotating. Since air resistance is proportional to the square of speed the windage power loss P_w is proportional to the cube of the rotational speed as

$$P_w = k_w \omega^3. \quad (2.35)$$

Efficiency map

When all the power losses are identified as functions of speed or torque they can be inserted into a function which describes the efficiency for the motor in every

operating point. The power delivered P_{out} by the motor is given by

$$P_{out} = T\omega , \tag{2.36}$$

and that the motor efficiency η_m is given by

$$\eta_m = \frac{P_{out}}{P_{in}} , \tag{2.37}$$

where P_{in} is the input power and therefore the output power plus the losses. If there are some constant losses C independent of speed and torque, like losses in electronic control circuits, this gives the motor efficiency as a function of speed and torque as

$$\eta_m = \frac{P_{out}}{P_{out} + losses} = \frac{T\omega}{T\omega + k_c T^2 + k_i \omega + T_f \omega + k_w \omega^3 + C} \tag{2.38}$$

By making a two dimensional contour plot of the motor efficiency function (2.38) it can easily be seen which operating points that is most efficient for the motor. In Figure 2.29 such a contour plot is exemplified together with the maximum torque and power limits discussed in Section 2.2.4. Since this model describes losses that occur in all motor types it can with other parameters also be used to plot efficiency maps for PM, Induction and SR motors [8].

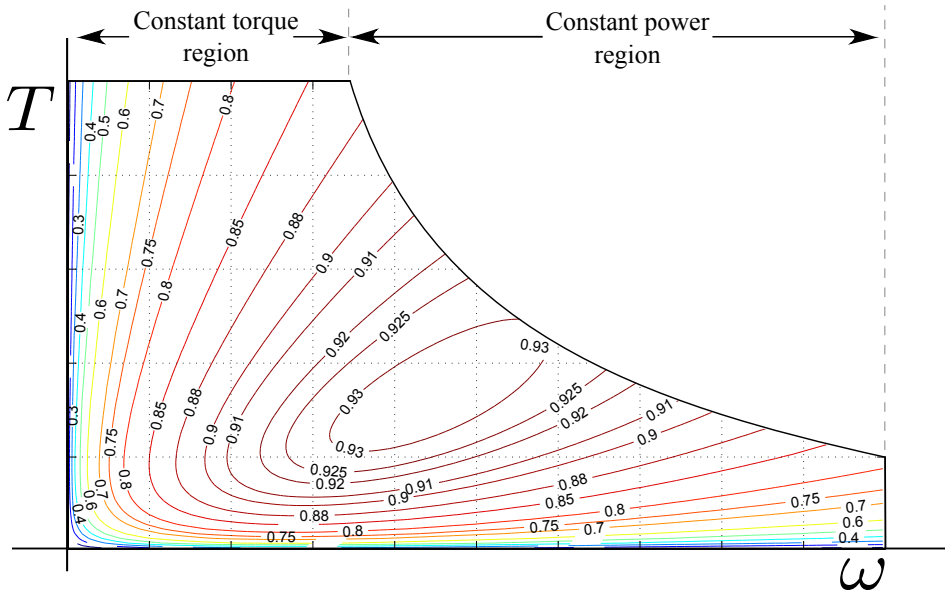


Figure 2.29. Example of efficiency map together with maximum torque and power limits for an undefined motor.

Chapter 3

Efficiency Map Generator

One big problem that arises when comparing different electric motors or when you want to simulate a vehicle using a specific motor is the lack of data. Information about the performance of a specific electric motor is often hard to get without performing measurements yourself which makes the data very expensive and time consuming to get hold of. This section describes a tool developed during the work to overcome this problem in a reasonable way.

3.1 Efficiency model

The efficiency maps of electric motors have a quite similar appearance as can be seen in Figure 1.3 and as it is explained in [8] the model (2.38) can be used to describe all the different motors quite well. The difference between the motor types is determined by the model parameters which heavily affects the efficiency map appearance. Therefore, here one model is used to generate missing data when some data is available independent of the machine type considered. After studying other electric motor efficiency models like the models in [13] and [14] the conclusion was that (2.38) gives the most satisfactory results regarding efficiency map appearance and is also very easy to fit to available efficiency map data since it is only dependant on torque and speed as variables.

3.1.1 Model adapted to data

If the model described by (2.38) is rewritten with minimal number of coefficients it becomes

$$\eta_m = \frac{T\omega}{T\omega + AT^2 + B\omega + C\omega^3 + D}, \quad (3.1)$$

which can describe all the losses discussed in Section 2.2. By using the least squares method for determining the coefficients of the model to fit measured data from a specific motor, in the form of efficiency values for different torque and speed, an efficiency map can be generated as in Figure 3.1 (a).

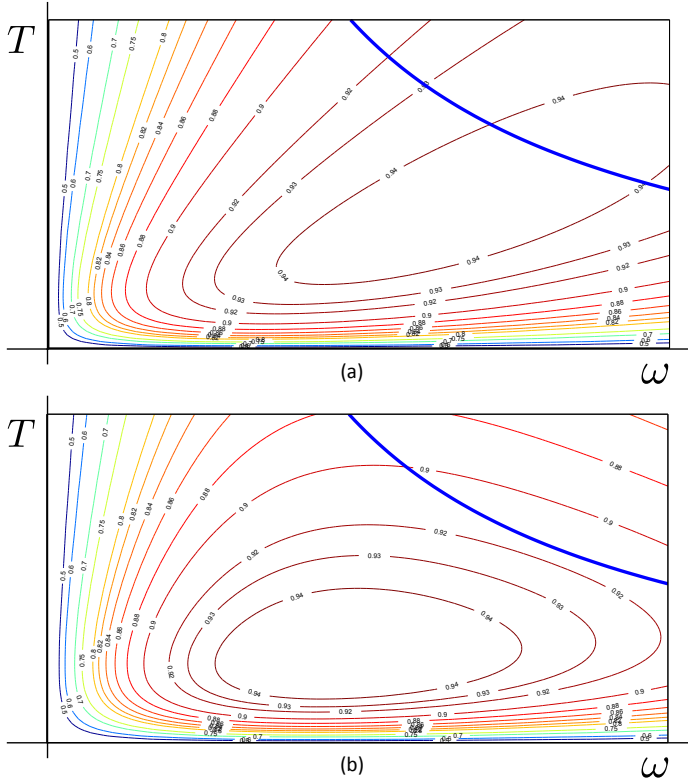


Figure 3.1. Model described by (3.1) in (a). The maximum power of the motor described by the blue line does not seem to affect the efficiency of the operating points. In (b) the modified model (3.2) is used.

It can be noticed that the efficiency map has a reasonable fit for low torque and speed, but for operating points close to maximum power the efficiency does not decline enough. Compare to e.g. the general appearance of the maps in Figure 1.3 where it can be seen that the efficiency declines when operating close to the maximum power of the motor. The reason for this is the losses described in (3.1) are only increasing with torque or speed. An attempt was thereby made to add losses depending on the power, i.e. $T\omega$. After trying different modifications of the model adapted to data the best solution was described by

$$\eta_m = \frac{T\omega}{T\omega + AT^2 + B\omega + C\omega^3 + D(T\omega - E)^2 + F}, \quad (3.2)$$

where a loss term including the square of the power is added. The square of the term is used to make the efficiency decline rapidly when getting close to the maximum power, the parameter D is determining the size of the loss term and the E parameter determines the relation to the maximum power limit of the motor. By adapting this modified model to the same data as was used to the original model

in Figure 3.1 (a) the generated efficiency map is quite different. In Figure 3.1 (b) the result of the least squares fit to the modified model can be seen, the efficiency now declines when operating close to the maximum power of the motor. The appearance of the efficiency maps in Figure 3.1 (a) and (b) is still similar at low torque and low speed operation. By comparing the result in Figure 3.1 (b) to Figure 1.3 it can be seen that a more typical appearance is achieved.

3.2 Data collection

An attempt to solve the lack of motor performance data was done by utilizing the information that often can be found published in articles or in product information sheets. This information often consists of images displaying the efficiency map of a motor or a set of measurements of efficiency for a few operating points. Since an image of the efficiency map basically contain all the information needed this is considered to be the best source of data. The challenge is to extract this information in an efficient way with high accuracy and also make it possible to use it together with the motor model (3.2) to get good approximations of data that e.g. can not be extracted. Data is often missing for low speed and torque because manufacturers usually leave that area empty in the efficiency maps.

3.2.1 Image reading

A tool is implemented that gives the user the ability to read the contours of an efficiency map in a fast and accurate way. The tool can be used on images of efficiency maps like the one in Figure 3.2 where the manufacturer have decided to show some of the efficiency contours and also the maximum torque curve. In this case speed and torque from 0 rpm and 0 Nm are included, but it is also, as stated in the previous section, common that the minimum values displayed starts at higher values.

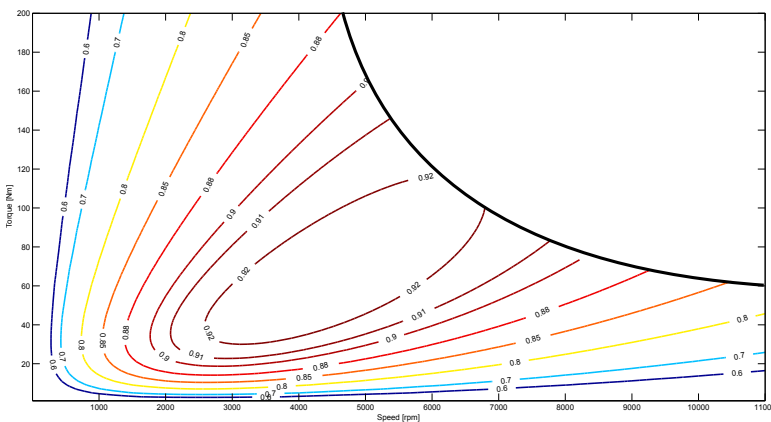


Figure 3.2. Example of the efficiency map appearance often seen among published motor performance information.

The procedure when using the tool starts by making a print screen of the efficiency map. The image is then to be cropped to only contain the map without the axes or anything outside the contours. When starting the tool it will ask for a .bmp, .png or .jpg file containing a cropped efficiency map. When the image is loaded the user will first have to enter the minimum and maximum speed and torque which are displayed on the original image. Then the user is asked for the efficiency contours that the image contains, this procedure can be seen in Figure 3.3 when done on the previous example.

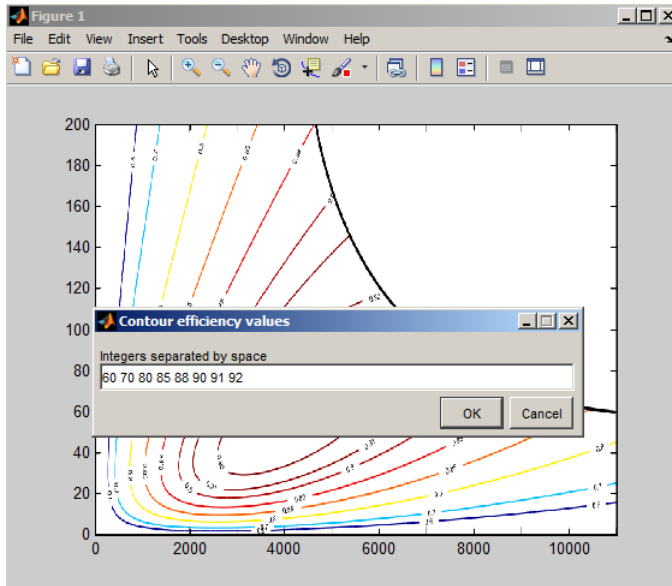


Figure 3.3. Image loaded and the values of the efficiency contours are specified.

When the tool has all the information about speed, torque and efficiency contours, the user can start to mark the contours on the image using the mouse. The contours are marked one by one starting with the number entered first in the dialogue box. When clicking on the contour a red circle will appear and the next click will draw a line to the next point and add a circle there too. This will mark the path of the contour in the coordinate system. When all the contours are marked the image will have the appearance of Figure 3.4. During this procedure also new information can be added as an improvisation by the user. This way of deviating from the contours can sometimes be used as a filter when it is obvious that there are some strange properties displayed.

The output data from the image reading can then be used to adapt the model (3.2) which gives the result in Figure 3.5. We can see that the result is very similar to the source in Figure 3.2 and now the efficiency information is available for all operating points in custom resolution instead of just being an image.

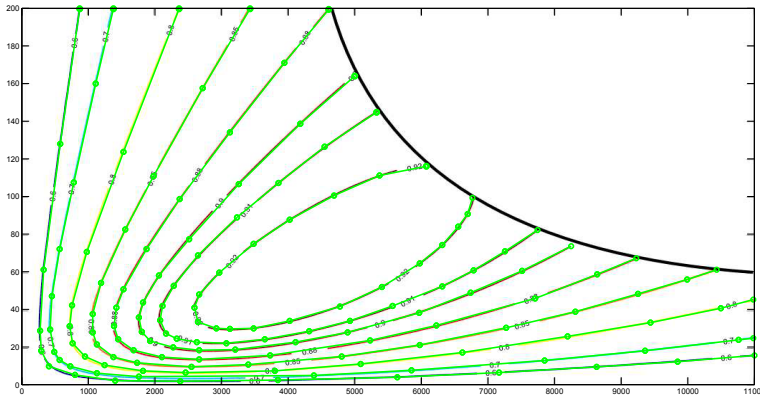


Figure 3.4. All the specified contours marked and information outside the maximum power area can be improvised.

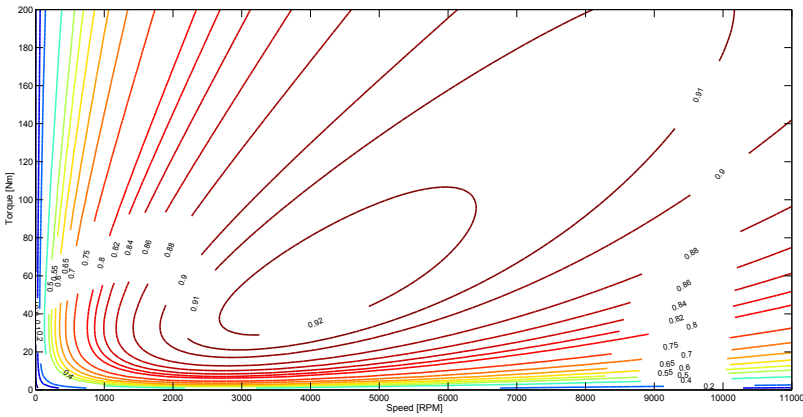


Figure 3.5. Model adapted to the data collected from the contour marking.

3.3 Creating efficiency maps

To make the creation of efficiency maps easy the Efficiency Map Generator (EMG) is implemented. It combines the electric motor model and the image reading tool with a lot of other functions to make it very convenient for the user to create an efficiency map with desired properties. The EMG GUI is displayed in Figure 3.6 and below there is a list of explanations for the different functions.

1. Load or Save data from workspace variable. Data has the format of a matrix with 3 columns and rows according to the number of data points.
2. Table displaying the data that is currently being processed by the tool.
3. Generate map takes data from the table and creates a surface by linear

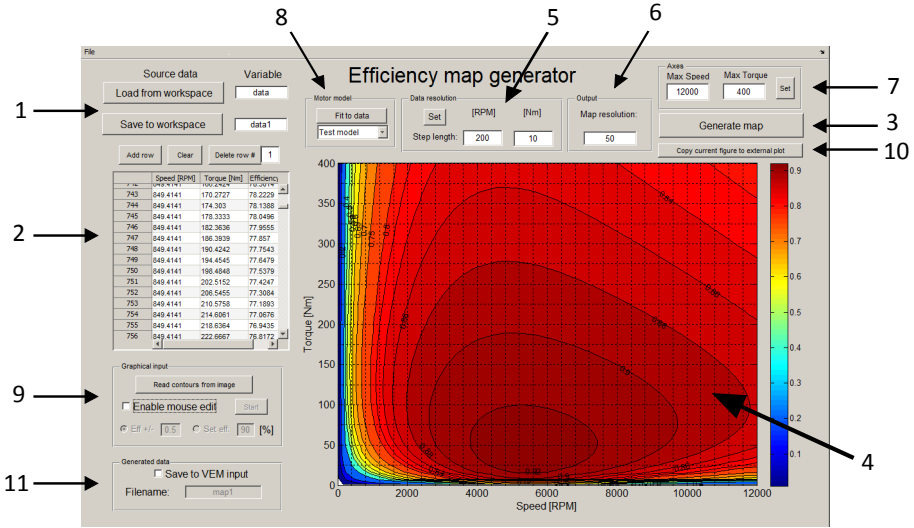


Figure 3.6. The Efficiency Map Generator during work on a random efficiency map.

interpolation between the points. The surface is then displayed as a contour plot.

4. Plot displaying the current state of the processed data/efficiency map.
5. Resolution of the data can be changed using linear interpolation.
6. Resolution per axis is set for the VEM file output.
7. Axes can be set for the plot.
8. The motor model can be used with three options
 - (a) Test model: Adapts the motor model to data in the table and displays the generated map without modification to the table.
 - (b) Fill gaps: Adapts the motor model to data in the table and uses the generated map data to fill gaps in a specified data set. The table is then replaced with the result.
 - (c) Replace table: Adapts the motor model to data in the table and replace the table with the generated data.
9. Graphical input can be done in two different ways
 - (a) Input to the table data using the plot and mouse. The user can modify the efficiency map by increasing/decreasing the efficiency at the operating point where the mouse is pointed. The user can also set the efficiency to a specified value. The computational burden often needs to be reduced by using the *Data resolution set* before using mouse input.

- (b) The image reading tool can be used to input data to the table. When pressing the button *Read contours from image* the user will be asked to load the image and when all the contours are marked the table will contain the marked contours as measured efficiency data points.
- 10. The current plot can be copied to an external figure to be able to easier compare modifications to the previous states.
- 11. When the user is satisfied with the created efficiency map it can be saved to VEM input data. If the check box is active the data is going to be saved in files when pressing *Generate map*.

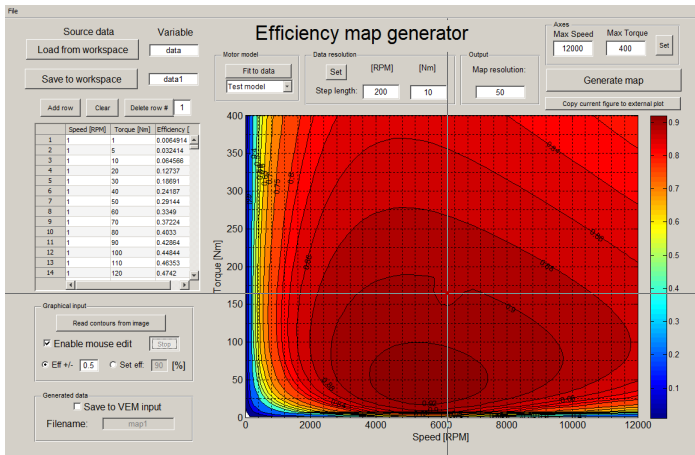


Figure 3.7. EMG during graphical input using the mouse. The efficiency has been reduced where the crosshair is located, compared to Figure 3.6. The current accuracy of 0.5 percentage unit can be changed in the edit box. Since a right-click was done in the figure the efficiency value where the crosshair is located is now 0.5 percentage units lower than before the click was performed.

3.4 Example of usage

This section demonstrates how the EMG can be used to generate an efficiency map to be used for simulation in VEM. In [15] the efficiency map of the Toyota Prius electric motor is displayed. By using the image of the map from the article and EMG, this motor can now be used in vehicle simulations with VEM.

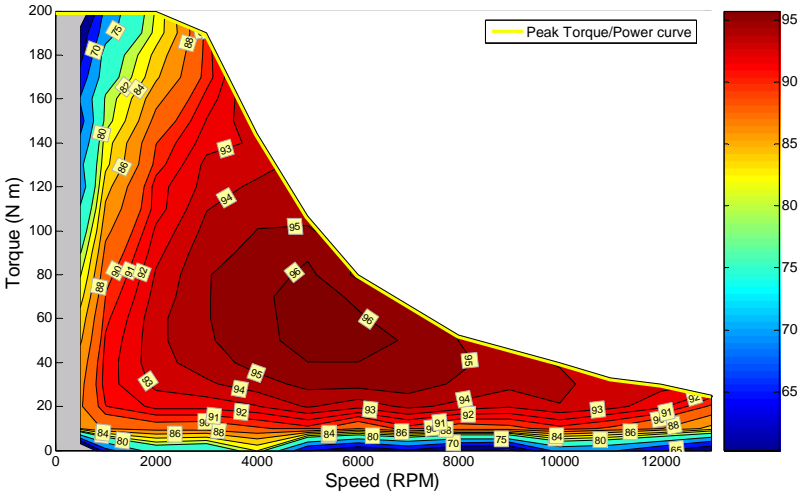


Figure 3.8. Toyota Prius efficiency map published in [15].

First the image of the efficiency map is made to a screenshot and then cropped to contain only the efficiency contours. The button *Read contours from image* is then pressed in the EMG and the cropped image is loaded. Since the motor model is not able to fit perfect to all electric motor efficiency maps in real life it has to be used where the benefit is the greatest. In this case there is a lot of data missing at low speed and the efficiency contours are also very dense at low speed and torque, so that is the area where the motor model is beneficial compared to contour reading because it is difficult to extract dense contour lines with high accuracy. The Toyota Prius efficiency map as seen in Figure 3.8 is therefore loaded into EMG image reading tool and the efficiency contours at low torque and speed are marked while the inner contours are only marked to some extent. This is a way to make the model fit as good as possible to the source data in the low speed and torque regions. The user decides where the border between inner and outer contours is, by trying different amount of marked contours a satisfactory result can be obtained and this is based on the resemblance with the original image. After adapting this data to the motor model a result as can be seen in Figure 3.9.

By studying the map generated by the model it can be seen that it does not look similar to the source regarding the high efficiency contours but it look good

at low torque and speed. This opens for the idea to edit the high efficiency operating points to fit better while keeping the outer points. By reading only the inner contours as seen in Figure 3.10 data is obtained as in Figure 3.11. And by using the *Fill gaps* function in EMG the model accuracy at low torque and speed can be combined with the image read accuracy of the high efficiency contours. This is done by creating a matrix of both the model efficiency data points and the inner high efficiency read contour points, the points in the model matrix is then replaced with the corresponding points in the high efficiency contour matrix. The *Fill gaps* functionality is demonstrated first in Figure 3.10 where the inner high efficiency contours of the efficiency map is marked. This extracted data is then displayed in Figure 3.11 where it can be seen that the "gap" that needs to be filled is everything around these high efficiency contours. This gap is then filled with the corresponding motor model data in Figure 3.9 to combine the best of the motor model with the best of the contour reading. After following this procedure the obtained result after the maximum torque limit is introduced can be seen in Figure 3.12. At this stage the efficiency map is ready to use for simulating the Toyota Prius electrical motor in the VEM. This creates the possibility simulating a specific real motor if an image of the efficiency map is available.

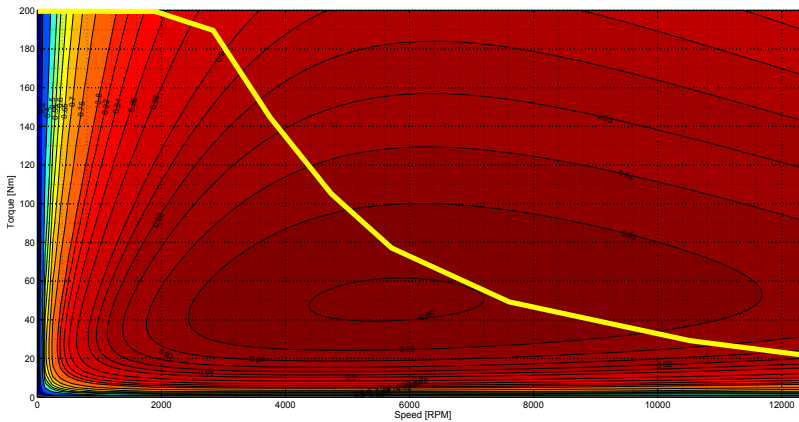


Figure 3.9. Motor model adapted to contours read from Toyota Prius efficiency map.

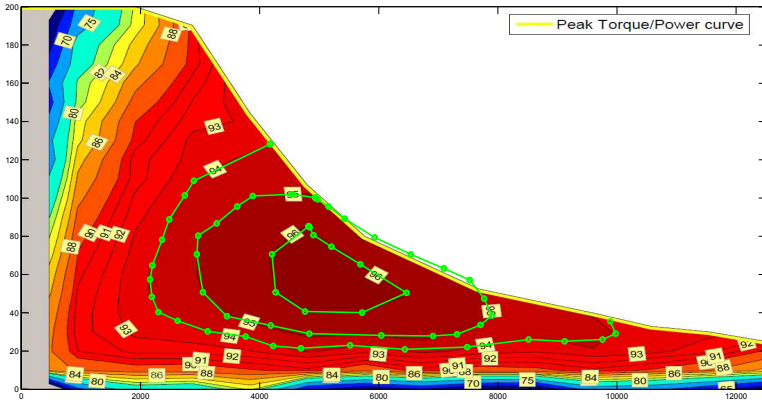


Figure 3.10. Inner efficiency map contours marked for the Prius motor.

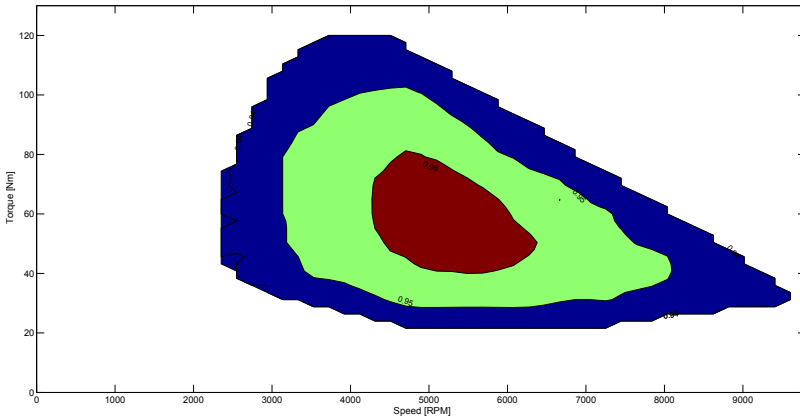


Figure 3.11. Data extracted from inner contours.

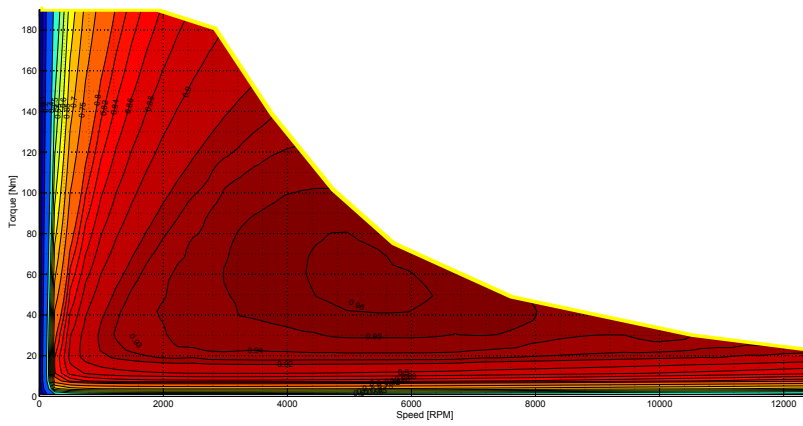


Figure 3.12. Toyota Prius efficiency map created in EMG.

Chapter 4

Electric Motor Performance Estimation Tool

When the EMG is available as a tool for collecting electric motor data it is possible to create models for each motor type based on this information. This is done in the Electric motor performance estimation tool along with methods of scaling these models to different sizes. The EPT is implemented as a Matlab script with a GUI as can be seen in Figure 4.1. The idea is that it should be possible to choose an electric motor type and the maximum power. The maximum torque curve together with efficiency map is then generated and saved as VEM input data files with the given name. Maximum torque and/or speed can be set to custom values lower than the tool default value for the generated motor. The tool default is set as a value considered to be the maximum possible for each motor type, hence only a lower limit is possible for the user to set.

4.1 Comparison of the electric motors

Since the EPT intend to clarify the differences between the different electric motors to assist in concept selection, the main source of information becomes comparative studies rather than electric motor modelling studies. It is determined that the motor model (3.2) is able to describe all the different motors, so the challenge is setting the parameters to describe the difference between the motors in a good way. The task of setting parameters by creating efficiency maps is quite straightforward after the implementation of EMG so the question is what kind of source that should be input for EMG to give reasonable results. To create a base for the EPT, this section summarizes different studies regarding electric motor selection for electric or hybrid vehicles.

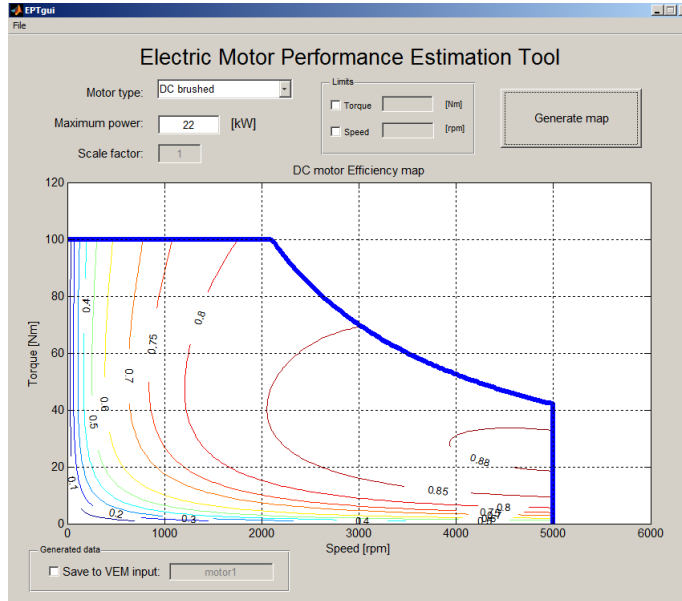


Figure 4.1. GUI for the EPT. A 22 kW brushed DC motor is generated and can be compared to the efficiency map of the 22 kW brushed DC motor displayed in [16] which is used as one of the sources to create the model.

4.1.1 General considerations

Power and torque limit

Higher rated speed leads to higher power density in electric motors, but also higher acoustic noise. This is because the size of the motor is deciding the possible output torque limit rather than the possible output power. Therefore high speed low torque motors can be small while delivering the same power as a high torque low speed motors as can be seen in Table 4.1.

Speed (rpm)	Mass (kg)
3000	270
1500	310
1000	415
750	570

Table 4.1. The rated speed and mass of several 37 kW induction motors from the same manufacturer [8].

Since the size of the motor decides the possible output torque the torque density can be defined as approximately constant values for different motor types. Table 4.2 gives an idea about what torque that is possible regarding the volume

and upper mass.

Motor type	$T/V_{envelope}$ (Nm/m ³)	T/CU mass (Nm/kg)
PM	28860	28.7-48
Induction	4170	6.6
SR	6780	6.1

Table 4.2. Typical torque density values for different motor types [17]. The PM motor with the permanent magnetic rotor field requires less induced field to produce torque than the other motors where the rotor lacks this property. Thereby the high amount of torque per copper for this motor type.

Efficiency

The efficiency of electric motors is also connected to the voltage level of the drivelines. High voltage rated drivelines are more efficient than lower voltage drivelines [3]. The cooling method also affects the efficiency, at lower temperatures the resistance of the windings is lower which results in less copper losses. Higher rated power leads to higher efficiency and thereby also higher power density. This can be summarized as that the more efficient motors also have higher power density. Since higher power contributes to higher efficiency the minimum requirement for high efficiency motors according to EU regulations is based on motor power. Table 4.3 show this behaviour for the Induction motor, the same thing can be observed for PM and SR motors but with 1-2% higher efficiency as explained in [8], but no tables corresponding to Table 4.3 could be found during this work.

Rated power (kW)	Minimum efficiency (%)
0.75	79.6
1.1	81.4
2.2	84.3
4	86.6
7.5	88.7
15	90.6
30	92.3
55	93.5
75	94.0
90	94.2
110	94.5
132	94.7
160	94.9
200	95.1
375	95.1

Table 4.3. The minimum efficiency at rated speed for IE2 (worldwide high efficiency standard) classified 4-pole Induction motors [18].

Higher speed motors are also more efficient than lower speed motors delivering the same power since the most important losses is due to torque which is proportional to current causing heat in the conductors. This also means that a motor should be as small as possible while delivering the required power if efficiency is the main priority [8].

4.1.2 DC motors

Brushed DC motors was once very popular for traction applications but are no longer considered a proper choice for most types of vehicles [2]. There are though still some applications where the brushed DC motor still is a good alternative to the modern vehicle types, since the cost can be lower and the performance still satisfactory [19]. In applications where the needed power is below 45 kW the brushed DC motor will still be competitive but in larger size the cooling of the rotor will become a problem [16]. Other motor types have most of their losses in the stator which makes cooling a lot easier for high power operation [8].

Good properties of the DC brushed motor is the very high torque at low speed and the good torque-speed characteristics for vehicle propulsion [11]. The torque response is also instantaneous even without the use of a controller and the overall control part of the brushed DC motor is very simple and cheap [4]. The reliability is also high since the technology is well established, which also contributes to lower prices. Bad properties of the brushed DC motor is the maintenance needs due to the wear of brushes, the low utilization factor of private vehicles though makes the coal brushes essentially maintenance free [3]. The efficiency, power density and maximum speed are also lower than the other motor types [4]. The power density problem is due to the difficulty of cooling the rotor in a compact motor while the efficiency and maximum speed limits are due to the friction of the brushed commutation.

4.1.3 Induction motors

Induction motors are together with PM motors the most common for electrical propulsion today. The shift from DC brushed motors became possible when the inverter which made it possible to control the induction motor in order to achieve variable speed operation needed for vehicle propulsion. For stationary usage where no variable speed controller is needed it is by far the most popular motor. The motor itself without the controller is an old invention and it is a very mature technology which is reliable and cheap. The lack of commutation makes it almost maintenance free [19]. The induction motors also have robust construction and high operating speed thanks to wide field weakening range. Especially for vehicles that requires a high-power motor the induction motor can be a more reliable choice than other motor types [2]. When machine size is increased the losses in the induction motor are not increased as much as in PM motors which makes it a good choice in vehicles where high performance is desired. The peak efficiency will probably be less than for the PM motors but the average efficiency may actually

be better [20].

The drawbacks of the induction motor is that the peak efficiency and torque density are in general lower than of the PM motor and SR motor. Induction motors also have limited torque capabilities at very low speed, this because at low speed the frequency of the stator field is low which leads to less induced current in the rotor [2]. The induction motor is more advanced to control than the other motor types, since it is harder to get stability over the whole torque-speed range and over temperature, which adds to the development cost, but likely little or no to production costs [20].

4.1.4 PM motors

The PM motor is a more modern technology than the DC brushed and the induction motor, but the control is basically the same as for the latter since if it is a synchronous machine it also needs a rotating stator field. This motor type is the most popular choice for electric vehicles and hybrid electric vehicles powertrain applications due to their high efficiency, high torque density, compact size, high torque at low speeds and easy control for regenerative braking [2]. If motors with the same peak efficiency are compared, the PM motors will be more efficient in overload transients at constant speed. The very high torque and power density makes the PM motor possible for use as in-wheel motors or other types where an extremely compact design is required [3]. Just like the induction motors the PM motors are virtually maintenance free since there is no brush that causes friction.

Even though there is no brush that limits the speed of the motor, the permanent magnet will limit the field weakening abilities of the motor which causes limited operating speed range [11]. The speed range can be improved in PM hybrid motors where an extra winding can make it possible for the controller to weaken the field of the permanent magnet, this naturally adds cost and complexity to the system [19]. There can be some problems with cogging torque in PM motors since the permanent magnet field is always active even if there is no current fed to the motor. Therefore some reluctance torque is still present depending when the current is removed, depending on the design of the rotor and stator. This can be solved and it is not a problem in other motor types. [4]. The permanent magnets of a PM motor can be sensitive to heat. This fact makes it very important to not overload a PM motor for too long since it can be demagnetized [2]. Time can also demagnetize the permanent magnets [4]. Rare earth materials for the magnets, and difficult manufacturing process makes the permanent magnets expensive and dependant on the supply of these rare materials. If the price of the permanent magnets gets lower the PM motors will also become cheaper and even more appealing for vehicle propulsion [8].

4.1.5 SR motors

The switched reluctance motor type is the most immature technology among the discussed in this work. It has been used in very few vehicles so far but it is by many people believed to become an very strong contender to induction and PM motors in the future. One of the most important features of the SR motors is the ability of very high speed operation. This is possible because of the robust rotor construction and the lack of brushes. Some small motors can achieve up to 30 000 rpm which gives very high power density [9]. For vehicle applications a motor speed over 10 000 rpm often is desirable, for PM motors there is a need for rotor modifications which increase cost and degrades efficiency to achieve this. Induction motors maximum speed is generally smaller than 10 000 rpm which gives the SR motor an advantage in this matter [11]. The cheap and robust construction also makes the SR motor excellent for use in hostile environments [16]. SR motors are slightly less efficient than PM motors but maintains efficiency over a wider range of speed and torque than any other motor type [8].

The switched reluctance motors have attracted attention in traction application due to their simple structure without squirrel cage or permanent magnets on the rotor which means lower losses than induction motors and no permanent magnetic fields that causes other problems [2]. Another advantage against permanent magnets is the ability to cope with high temperatures [3]. All these prominent advantages makes the SR motors very attractive for vehicle applications. But since they are not yet produced as standard motors they are still more expensive than the other types [21]. Some of the disadvantages with SR motors is high acoustic noise, torque ripple and advanced converter technology. With these problems solved the SR motors will be ideally suited for vehicle propulsion [4].

4.1.6 Motor property ratings

Several authors of work regarding motor selection for vehicles have given the different motor types relative grades regarding each important factor. This section describes the different sources and makes a summary that can be used for modelling the different types.

Efficiency

Since efficiency plays a key role in this work it is extracted from the sources and compared. In Table 4.4 the relative ratings for each motor type efficiency is displayed. All the sources agree that DC is the least efficient and that PM is the most efficient of the different motor types. The battle between Induction and SR for the middle spots is a even, since some sources suggest that they are equally efficient. But judging from the average and by taking other statements into account the conclusion in this summary is that the SR motor is generally more efficient than the Induction motor.

The different authors grade different properties among the motors, the only common property is efficiency which made it easy to compare. Their conclusions

Source	DC	Induction	PM	SR
[22]	2	6	8	6
[3]	2	3.5	5	4
[11]	2	4	5	4.5
[23]	2.5	3.5	5	3.5

Table 4.4. Relative grades for efficiency given to each motor type by different sources. Higher number is better efficiency according to all grading systems. Each line compares the motor types independent of the others.

about which is the "best motor for vehicle propulsion" can though be interesting to address since all the motor types except for DC brushed were considered the best option depending on the author.

4.2 Motor type parameter selection

This section describes how the different electric motor types efficiency map parameters and torque curves are determined for use in EPT using the discussion in Section 4.1 and other resources.

4.2.1 Efficiency scaling

Since the efficiency depends on the power of the electric motor this should be taken into account when determining the average efficiency maps. In Table 4.3 the behaviour of the maximum efficiency can be observed when the motor size is increased. If this data is used to adapt a power function, which turned out to give the best fit, on the form

$$f(x) = ax^b + c \quad (4.1)$$

the coefficients $a = -18.56$, $b = -0.2762$ and $c = 99.43$ gives the fit as seen in Figure 4.2.

This maximum efficiency for induction motors as a function of the motor size can now be used for scaling the motors continuously from around 1 kW to over 200 kW and get a realistic maximum efficiency of the efficiency maps. Since the maximum value for efficiency in Table 4.3 is 95.1 % and obtained for both 200 kW and 375 kW it should be considered as the maximum for the function. By modifying the power function (4.1) to have 95.1 as maximum value we get

$$f(x) = \min(-18.56x^{-0.2762} + 99.43, 95.1), \quad (4.2)$$

which can be used as an estimation of the maximum efficiency for the induction motors of all different sizes. Since this should give a 1-2% lower efficiency than for PM and SR motors the efficiency for them can be obtained by adding between 1 and 2 percent units to the function (4.2). To achieve the correct efficiency for the DC brushed motors the value will have to be lowered since their efficiency is considered to be lower than for the induction motors.

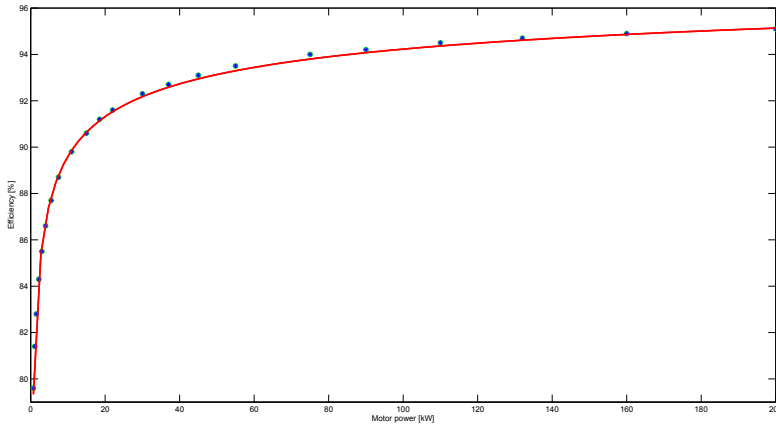


Figure 4.2. Data points from Table 4.3 displayed together with the power function in red.

4.2.2 DC motor

To design the efficiency map and the maximum torque curve for the brushed DC motors the visual characteristics of the efficiency map is studied from different sources and summarized into one map that was created in EMG. All the studied sources show the same type of appearance for the DC brushed motors. After comparison with the efficiency for the brushed DC motors displayed in [16] and [24] the decision was to subtract the calculated maximum efficiency in (4.2) by 3.5 percent units to get a reasonable value for brushed DC motors. To make sure that the appearance of the efficiency map was correct regarding the relative position of the maximum efficiency area and the distribution of the efficiency contours the efficiency maps in [8] and [3] was also taken into account. The maximum torque curve is also designed by putting the different sources together. When scaling the efficiency map both the torque and speed axis is scaled equally to achieve the correct amount of maximum power, this scaling method is also used for the other motor types. Examples of generated DC motor efficiency maps can be seen in Figure 4.3 and Figure 4.4.

4.2.3 Induction motor

The parameter selection of the Induction motor is more difficult than for the DC brushed motor. The reason to this is that the induction motor have characteristics that can differ more between one motor to the other. The characteristics is also similar to those of the PM motors. To be able to distinguish the induction motor from the PM motor it is modeled according to the discussion in [25] and [3]. This together with the speed limit discussed in Section 4.1 and the efficiency scaling (4.2) gives the result in Figure 4.5 and Figure 4.6. This can be compared to the map displayed in [26] which is the only officially published map for an induction motor in a vehicle application that could be found during this work.

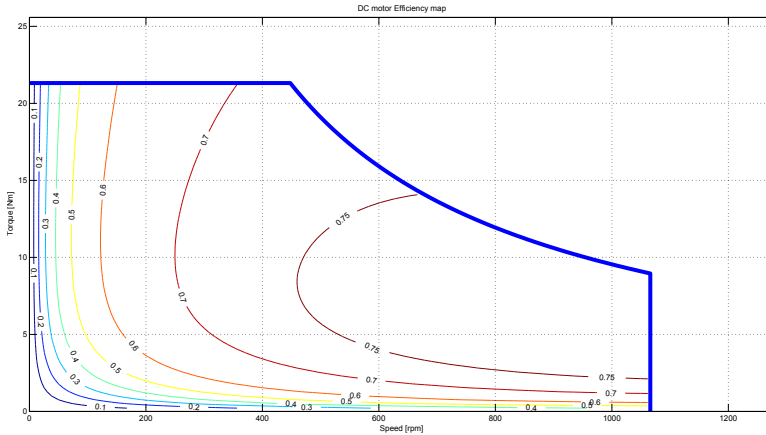


Figure 4.3. 1 kW DC brushed motor efficiency map and torque curve generated.

4.2.4 PM motor

Since the PM motor has been a very popular motor choice recently there is more information found about the efficiency map appearance than for the induction motor. When determining the efficiency map for the PM motors the general discussions in [3] and [25] was combined with the real cases of [15] and [27] as source information. To get the highest maximum efficiency of any motor type 2 percent units is added to the efficiency scaling equation (4.2). It can also be beneficial to use manual limits for maximum torque and speed for the PM motor type since these can vary significantly between different specific models of PM motors. Examples of generated PM motor efficiency maps can be seen in Figure 4.7 and Figure 4.8.

4.2.5 SR motor

Studies of the SR motor type included comparing many different sources of information regarding the SR motor torque curve and efficiency map. Every source available agreed that the SR motor is most efficient at very high speed and that the efficiency is still high over a large range of the efficiency map. This is described by general discussions in [28], [25] and [3], and it is also confirmed by real SR motors in [29], [30] and [31]. In [12] and [19] it is also described that the maximum speed is high compared to other motor types, up to 7 times the base speed. To get a maximum efficiency between that of the induction motor and the PM motor, 1 percent unit is added to the efficiency scaling function (4.2). Examples of generated PM motor efficiency maps can be seen in Figure 4.9 and Figure 4.10.

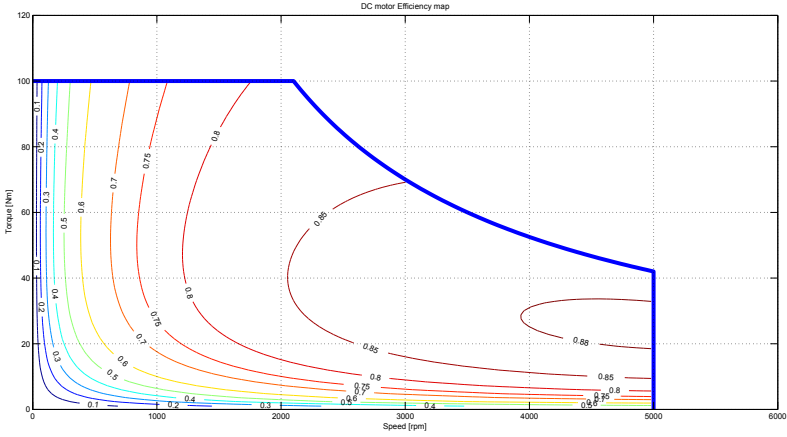


Figure 4.4. 22 kW DC brushed motor generated, efficiency is higher than for the motor in Figure 4.3.

4.2.6 Motor model parameters validation

Since there is a lack of measurement data of different motor types and sizes these model parameters or the efficiency scaling could not be validated properly during this work. The only way to be sure the models and the generated efficiency maps represent their respective motor type is to study the source information referred to in this text or other available motor data.

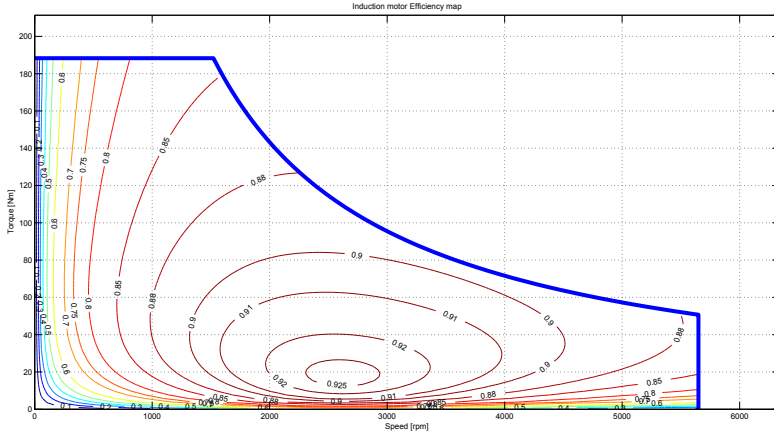


Figure 4.5. 30 kW Induction motor efficiency map and torque curve generated.

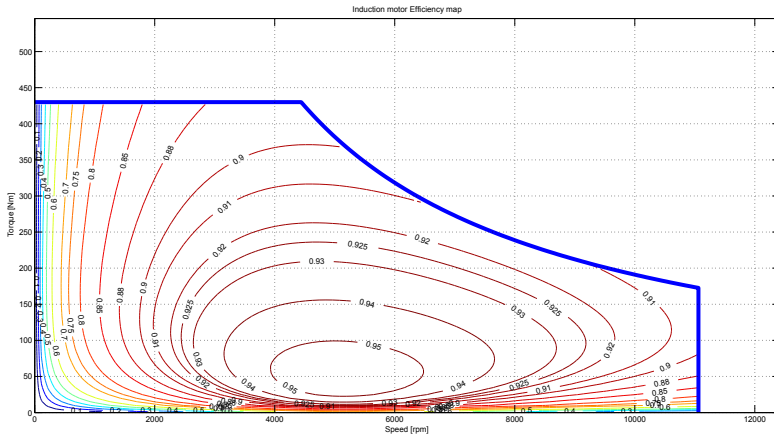


Figure 4.6. 200 kW Induction motor efficiency map generated. The efficiency is slightly higher than for the motor in Figure 4.5.

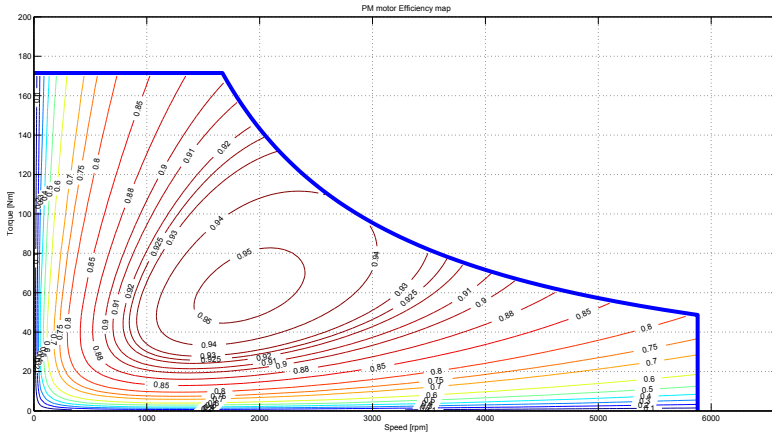


Figure 4.7. 30 kW PM motor efficiency map and torque curve generated.

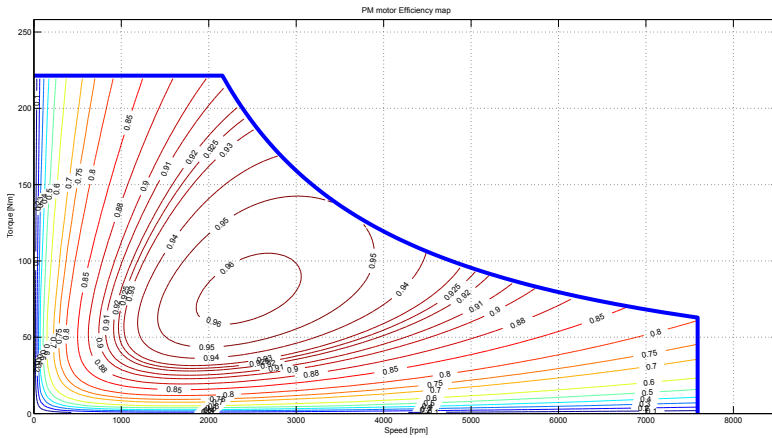


Figure 4.8. 50 kW PM motor generated. The torque curve has the same profile as the 50 kW PM motor displayed in [8].

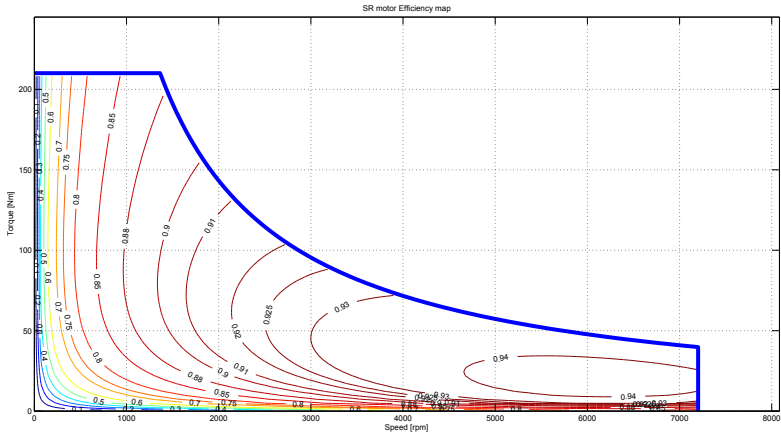


Figure 4.9. 30 kW SR motor efficiency map and torque curve generated.

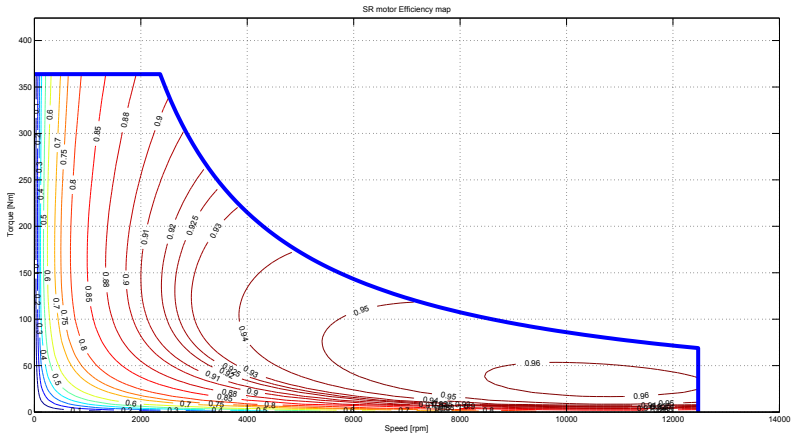


Figure 4.10. 90 kW SR motor generated, high speed operation possible.

4.3 Generating VEM data

When the efficiency map and torque curve are generated in the desired way they should be converted to fit the input of the VEM. Since the VEM is simulating both motoring and generating mode of the electric motor the efficiency map has to be expanded to also cover negative torques. There are two ways conceptually possible in order to extend the motor mode to also cover generator mode discussed in [13]. Here the chosen method is to calculate the losses in the motor mode and then mirror the losses to the generator side of the speed axis. This method is chosen since the expression for the efficiency (3.2) can be written as

$$\eta_m(\omega, T) = \frac{T\omega}{T\omega + losses(\omega, T)}, \quad (4.3)$$

where the term *losses* can be approximated as having the same value for negative and positive torque of the same size for the same speed. This gives

$$losses(\omega, T) = \frac{1 - \eta_m(\omega, T)}{\eta_m(\omega, T)} T\omega, \quad (4.4)$$

which can be calculated for the motoring part using the efficiency maps generated. The losses are then mirrored by performing

$$losses(\omega, -T) = losses(\omega, T), \quad (4.5)$$

and the losses for both motoring and generating mode is obtained as can be seen in Figure 4.11.

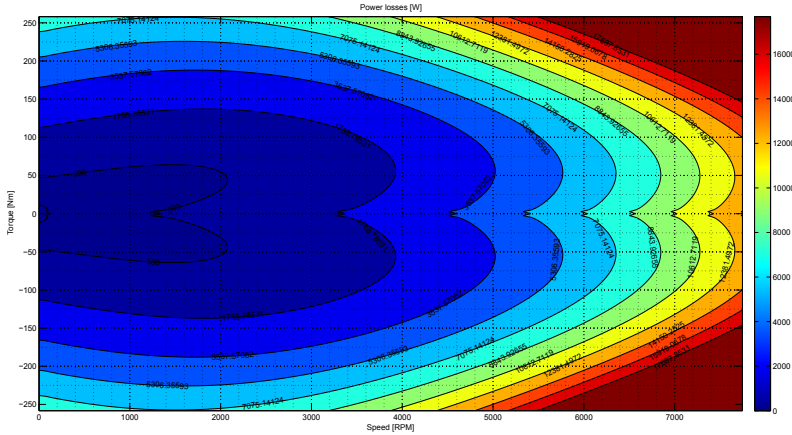


Figure 4.11. Power losses for the 50 kW PM motor in Figure 4.8 now in both motoring and generating mode.

The electric motor input to VEM has the format of actual needed electric power for each operating point. This means that the output power has to be added to the losses in Figure 4.11 by performing the following equation valid both for motoring

and generating mode since the electric power and output power are both negative on the generator side

$$P_{electric} = P_{out} + losses = T\omega + losses , \quad (4.6)$$

which transforms Figure 4.11 into Figure 4.12 where we can see the electric power the motor uses to deliver each operating point. The

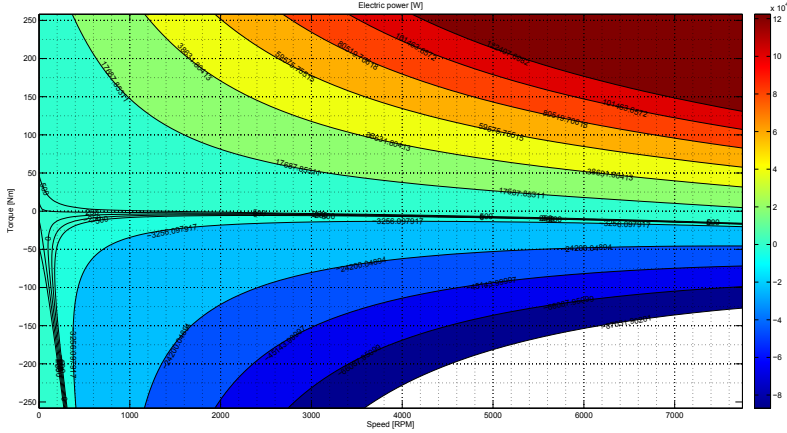


Figure 4.12. Electric power for the 50 kW PM motor. We can see that the electric power is negative in most of the negative torque area which means that regenerative braking is possible. We can also see that we have some positive power at zero torque which means the motor needs power to rotate without load.

4.4 Simulations in VEM

To verify that the data generated by EPT is reasonable and also compatible with VEM some simulations are performed. A regular pure electric vehicle with specifications as in Table 4.5 are configured in VEM with the possibility to change the electric motor. The car chassis is modeled by the coast down coefficients methodology described in [32]. The electric motor is connected to the wheels through a single-speed gearbox with 98% efficiency, and the gear ratio can also be varied.

Three 90 kW motors are generated according to the motor model parameters presented earlier in this chapter, one for each of the most interesting motor alternatives, Induction, PM and SR. Two different gear ratios, 3 and 8, are first simulated to illustrate the differences between the different motors and what impact the gear selection has on the performance and efficiency of the vehicle. Different drive cycles are also used in the simulations to investigate if there are any differences regarding usage for the motors. To test city and highway conditions separately the NEDC drive cycle [33] is used and divided into the urban and extra urban parts before simulating.

When gear ratio 3 is used the PM motor is the most efficient. All of the motors have the same top speed which means that it is the maximum power which

Parameter	Value	Unit
Total mass	1590	<i>kg</i>
Wheel radius	0.3	<i>m</i>
Wheel inertia	2	<i>kgm²</i>
Rolling resistance	133	<i>N</i>
Rotating friction	3	$\frac{N}{m/s}$
Aerodynamic drag	0.3	$\frac{N}{(m/s)^2}$
Auxiliary load	300	<i>W</i>

Table 4.5. Parameters for the electric vehicle simulated in VEM.

	IM90kW	PM90kW	SR90kW
Average consumption			
Urban [kWh/10km]	1.63	1.51	1.72
Extra urban [kWh/10km]	1.38	1.30	1.43
Performance			
0-50 [sec]	7.5	8.3	6.7
0-100 [sec]	15.3	16.9	13.7
Top speed [km/h]	220	220	220

Table 4.6. Simulation of vehicle described by Table 4.5 with gear ratio 3.

sets the limit for the speed, 220 km/h is a realistic top speed for a 90 kW motor. With higher maximum torque the SR motor has the best acceleration performance but still the worst efficiency since the operation points used is far from maximum speed, which also means average torque. By plotting the operation points together with the efficiency map as in Figure 4.13 and Figure 4.14 it is easy to see why this is a reasonable result.

By increasing the gear ratio to 8 higher speeds of the motor will be used as well as lower torque. We can now see that the maximum speed of the motors is limiting the top speed of the vehicle which makes it lower than in the previous simulation. This is beneficial for the SR motor because of its higher speed limit and high efficiency at high speed. Since the motors now operate on higher speed and lower torque both the induction and the SR motor becomes more efficient than the PM motor. The changed gear ratio also improved the acceleration performance of all the motor alternatives.

By studying Figure 4.13 we can see that the gear ratio 3 makes the highest speed operating points being located to the maximum efficiency area which explains the low energy consumption for extra urban driving. If the efficiency should be optimized for highway cruising the gear ratio 3 would be a very good choice for the 90 kW PM motor. When the gear ratio was increased to 8 the maximum efficiency area never was used and the consumption got higher for both urban and extra

	IM90kW	PM90kW	SR90kW
Average consumption			
Urban [kWh/10km]	1.24	1.78	1.42
Extra urban [kWh/10km]	1.31	1.60	1.30
Performance			
0-50 [sec]	2.8	3.0	2.6
0-100 [sec]	8.6	8.8	8.4
Top speed [km/h]	139	145	177

Table 4.7. Simulation of vehicle described by Table 4.5 with gear ratio 8.

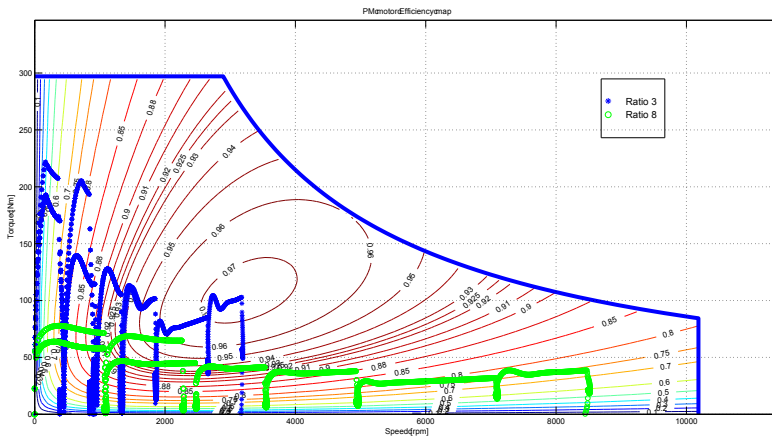


Figure 4.13. The 90 kW PM motor and the NEDC operating points for gear ratio 3 in blue and 8 in green. The high speed extra urban points are in the higher speed of the same color as the urban points at lower speeds. When changing gear ratio to a higher value we can see that the operating points get stretched along the speed axis and compressed along the torque axis.

urban.

The SR motor has the maximum efficiency at higher speed and lower torque than the PM motor as can be seen when comparing the two efficiency maps. In Figure 4.14 the operating points for gear ratio 3 and 8 are plotted just like for the PM motor. We can see that the maximum efficiency area is never used with any of these gear ratios so there is still potential for improvement. To illustrate how the SR motors properties can be used even better a third gear ratio was simulated. This ratio had to be higher than 8 to reach the higher speeds so ratio 10 was chosen. In Figure 4.14 it can be seen how ratio 10 is using the maximum efficiency area for the SR motor during extra urban driving which should reduce the energy consumption further.

In Table 4.8 the results of gear ratio 10 for the SR motor is displayed. The consumption for both urban and extra urban is lower than for the PM motor using

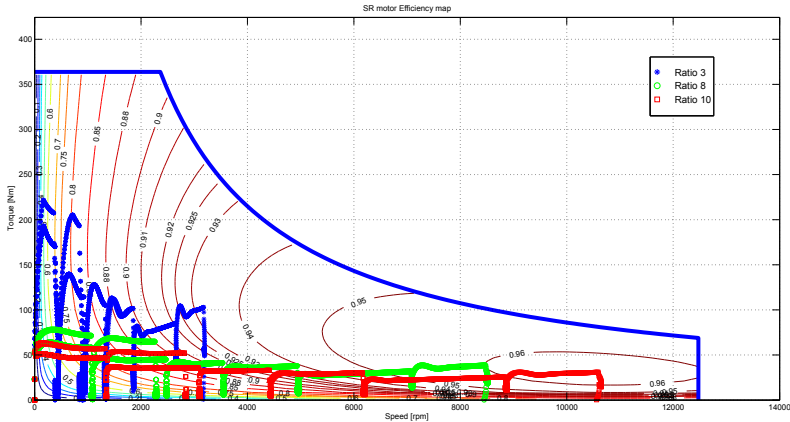


Figure 4.14. The 90 kW SR motor correspondent to Figure 4.13. Gear ratio 10 in red is added to achieve better efficiency and performance.

SR90kW	
Average consumption	
Urban [kWh/10km]	1.37
Extra urban [kWh/10km]	1.27
Performance	
0-50 [sec]	2.3
0-100 [sec]	8.1
Top speed [km/h]	142

Table 4.8. Simulation of vehicle described by Table 4.5 with gear ratio 10 for SR motor only. The lower maximum speed for the PM motor prevents it from following the NEDC drive cycle using gear ratio 10.

ratio 3. The performance achieved when using gear ratio 10 with the SR motor is also very impressive, the acceleration is now significantly better than for gear ratio 3. This means that the vehicle can achieve both good efficiency and performance when using the SR motor and a carefully selected gear ratio, while these two properties are more difficult to combine for the PM motor.

When looking at the plots of operating points on the efficiency maps it can be easy to think that the motors are oversized for the application. Since the NEDC drive cycle is using low power the most efficient motor choice would be a small motor which works in the high efficiency area more often than a bigger motor. The drawback of this is that the vehicle also needs to have some kind of acceleration performance which the small motor can not deliver. One way of handling this problem would be to use a two motor solution where both motors work during acceleration and only one motor during highway cruising or other low power driving conditions.

Chapter 5

Conclusions and future work

In this chapter the conclusions from the work is presented together with suggestions for future work.

5.1 Conclusions

Two tools have been created to assist in the analysis of electric motors in vehicle propulsion systems. The initial goal of creating a tool for estimating the typical performance properties for different electric motors was extended to also cover a solution to the problem of collecting motor data. Now, when the EMG tool has been implemented along with EPT the opportunity has arisen to use information found about electric motors such as images of efficiency maps or measured efficiency for some operating points, and also simulate a vehicle using this motor data. This brings greater opportunities for the one who is performing concept selection studies. The possibility to create a big library of electric motor data for real electric motors with documented properties by using EMG is probably even more important than the creation of the average motor efficiency maps. This because the average motor models are a simplification of the reality that results in all the motors of a certain type and size has the same properties which is not the case in reality. These models are however useful when making a rough comparison between motor types before going into detailed comparison between specific motors. The average models for each motor type might even be better suited to describe motors of specific characteristics in general rather than DC, IM, PM or SR motors. This since for instance a PM and an IM motor can have almost exactly the same efficiency map and maximum torque curve if the manufacturer design the motors in a way to achieve this. Thereby it might be better to compare motors of certain characteristics rather than different motor types. The study can then be performed to compare a motor that has maximal efficiency at high speed and low torque against a motor that has maximum efficiency at average speed and torque instead of saying that this comparison is between e.g. a PM and a SR motor. This work is also a good summary of information that is of importance when discussing motor selection with references to many motor selection studies

where deeper knowledge can be obtained if desired. This should make the report a good read before or during the motor selection process. If the reader has little knowledge about electric motor design and operation this report also handles these topics regarding the DC, Induction, PM and SR motor types.

5.2 Future work

Since there is now a base for creating efficiency maps from different sources of information, work can be done in both collecting this information, but also use it to improve other parts of the work. The EMG can presently be used to collect data and make a library of different electric motors to make the available options as many as possible when conducting the concept selection process. Improvements can especially be done when more data gets available or when there is a possibility to perform measurements on motors. The efficiency maps created in EMG could then be validated in a greater extent and the same could be done with the average efficiency maps for the different motor types to control how reliable the generated efficiency maps are for different motor sizes and motor types. The model of the induction motor should also be investigated further since it is the one which has used the least information when created.

Bibliography

- [1] C.C. Chan and K.T. Chau. *Modern Electric Vehicle Technology*. Oxford University Press, 2001. ISBN13 978-0198504160.
- [2] Chris Mi, M. Abul Masrur, and David Wenzhong Gao. *Hybrid Electric Vehicles Principles and Applications with Practical Perspectives*. John Wiley and Sons, 2011. ISBN13 978-1119998907.
- [3] J. de Santiago, H. Bernhoff, B. Ekergård, S. Eriksson, S. Ferhatovic, R. Waters, and M. Leijon. Electrical motor drivelines in commercial all-electric vehicles: A review. *IEEE Transactions on Vehicular Technology*, 61(2), Feb 2012.
- [4] Iqbal Husain. *Electric and Hybrid Vehicles Design Fundamentals*. CRC Press, 2 edition, 2010. ISBN13 978-1439811757.
- [5] Sune Söderkvist. *Kretsteori och Elektronik*. Linköpings Universitet, 4 edition, 2005.
- [6] David K Cheng. *Field and Wave Electromagnetics*. Addison-Wesley, 2 edition, 1989. ISBN 9780201528206.
- [7] A.E. Fitzgerald, Jr. Charles Kingsley, and Stephen D. Umans. *Electric Machinery*. McGraw Hill Higher Education, 2 edition, 2002. ISBN13 9780071230100.
- [8] James Larminie and John Lowry. *Electric Vehicle Technology Explained*. John Wiley and Sons, 2 edition, 2012. ISBN13 978-1119942733.
- [9] Austin Hughes. *Electric Motors and Drives*. Newnes (an imprint of Butterworth-Heinemann Ltd), 3 edition, 2006. ISBN13 9780750647182.
- [10] K.T. Chau, C.C. Chan, and Chunhua Liu. Overview of permanent-magnet brushless drives for electric and hybrid electric vehicles. *IEEE Transactions on Industrial Electronics*, June 2008.
- [11] X.D. Xue, K.W.E. Cheng, and N.C. Cheung. Selection of electric motor drives for electric vehicles. *Power Engineering Conference*, 2008.

- [12] Z.Q. Zhu and David. Howe. Electrical machines and drives for electric, hybrid, and fuel cell vehicles. *Proceedings of the IEEE*, April 2007.
- [13] Lino Guzzella and Antoni Sciarretta. *Vehicle Propulsion Systems - Introduction to Modeling and Optimization*. Springer Verlag, 2 edition, 2007. ISBN13 978-3540746928.
- [14] Cui Shumei, Liang Chen, and Song Liwei. Study on efficiency calculation model of induction motors for electric vehicles. *IEEE Vehicle Power and Propulsion Conference (VPPC), Harbin, China*, September 3-5 2008.
- [15] T.A. Burress, S.L. Campbell, C.L. Coomer, C.W. Ayers, A.A. Wereszczak, J.P. Cunningham, L.D. Marlino, L.E. Seiber, and H.T. Lin. Evaluation of the 2010 toyota prius hybrid synergy drive system. *Oak Ridge National Laboratory*, March 2011.
- [16] Ron Hodkinson and John Fenton. *Lightweight Electric/Hybrid Vehicle Design*. SAE International, 2001. ISBN13 978-0750650922.
- [17] Yimin Gao, M. Ehsani, and J.M. Miller. Hybrid electric vehicle: Overview and state of the art. *IEEE ISIE*, June 2005.
- [18] Energimyndigheten. Om klassificering och märkning, energimyndighetens lista över högeffektiva elmotorer. <http://energimyndigheten.se/sv/Foretag/Energieffektivisering-i-foretag/Tillverkningsindustri---hjalpsystem-och-processer/Elmotorer/Energimyndighetens-lista-over-hogeffektiva-elmotorer/>, March 2010.
- [19] Mounir Zeraoulia, Mohamed El Hachemi Benbouzid, and Demba Diallo. Electric motor drive selection issues for hev propulsion systems: A comparative study. *IEEE Transactions on Vehicular Technology*, November 2006.
- [20] Wally Rippel. Induction versus dc brushless motors. <http://www.teslamotors.com/blog/induction-versus-dc-brushless-motors>, January 2007.
- [21] C.C. Chan. The state of the art of electric, hybrid, and fuel cell vehicles. *Proceedings of the IEEE*, April 2007.
- [22] Allen Fuhs. *Hybrid Vehicles and the Future of Personal Transportation*. Taylor and Francis, 2008. ISBN13 978-1420075359.
- [23] C.C. Chan and Y.S. Wong. The state of the art of electric vehicles technology. *The 4th International IPEMC.*, 2004.
- [24] W.L. Soong. Dc machines : Parameter measurement and performance prediction. *Power Engineering Briefing Note Series*, May 2008.
- [25] S.M. Lukic and A. Emado. Modeling of electric machines for automotive applications using efficiency maps. *Electrical Insulation Conference and Electrical Manufacturing and Coil Winding Technology Conference*, 2003.

- [26] A.N. Brooks and T.B. Gage. The tzero electric sports car: How electric vehicles can achieve both high performance and high efficiency. *AC Propulsion*, May 2000.
- [27] Hans Kemper, Gereon Hellenbroich, and Thomas Esch. Concept of an innovative passenger-car hybrid drive for european driving conditions. *FEV Motorentchnik Aachen*, September 2009.
- [28] J.G.W. West. Dc, induction, reluctance and pm motors for electric vehicles. *IEEE Colloquium on Motors and Drives for Battery Powered Propulsion*, April 1994.
- [29] Zhang Qianfan, Liu Xiaofei, Cui Shumei, Dong Shuai, and Yu Yifan. Hybrid switched reluctance motor and drives applied on a hybrid electric car. *Harbin Institute of technology*, 2011.
- [30] K.M. Rahman and S.E. Schulz. Design of high-efficiency and high-torque-density switched reluctance motor for vehicle propulsion. *IEEE Transactions on Industry Applications*, 2002.
- [31] A. Chiba, Y. Takano, M. Takeno, T. Imakawa, N. Hoshi, M. Takemoto, and S. Ogasawara. Torque density and efficiency improvements of a switched reluctance motor without rare-earth material for hybrid vehicles. *IEEE Transactions on Industry Applications*, 2011.
- [32] E. Galvagno and A. Vigliani. A numerical model for evaluating seal friction effects on automotive driveline performances. *International Conference on Tribology*, September 2006.
- [33] Wikipedia. New european driving cycle. http://en.wikipedia.org/wiki/New_European_Driving_Cycle.

Upphovsrätt

Detta dokument hålls tillgängligt på Internet — eller dess framtida ersättare — under 25 år från publiceringsdatum under förutsättning att inga extraordinära omständigheter uppstår.

Tillgång till dokumentet innebär tillstånd för var och en att läsa, ladda ner, skriva ut enstaka kopior för enskilt bruk och att använda det oförändrat för icke-kommersiell forskning och för undervisning. Överföring av upphovsrätten vid en senare tidpunkt kan inte upphäva detta tillstånd. All annan användning av dokumentet kräver upphovsmannens medgivande. För att garantera äktheten, säkerheten och tillgängligheten finns det lösningar av teknisk och administrativ art.

Upphovsmannens ideella rätt innefattar rätt att bli nämnd som upphovsman i den omfattning som god sed kräver vid användning av dokumentet på ovan beskrivna sätt samt skydd mot att dokumentet ändras eller presenteras i sådan form eller i sådant sammanhang som är kränkande för upphovsmannens litterära eller konstnärliga anseende eller egenart.

För ytterligare information om Linköping University Electronic Press se förlagets hemsida <http://www.ep.liu.se/>

Copyright

The publishers will keep this document online on the Internet — or its possible replacement — for a period of 25 years from the date of publication barring exceptional circumstances.

The online availability of the document implies a permanent permission for anyone to read, to download, to print out single copies for his/her own use and to use it unchanged for any non-commercial research and educational purpose. Subsequent transfers of copyright cannot revoke this permission. All other uses of the document are conditional on the consent of the copyright owner. The publisher has taken technical and administrative measures to assure authenticity, security and accessibility.

According to intellectual property law the author has the right to be mentioned when his/her work is accessed as described above and to be protected against infringement.

For additional information about the Linköping University Electronic Press and its procedures for publication and for assurance of document integrity, please refer to its www home page: <http://www.ep.liu.se/>